A LASER VELOCIMETER TO STUDY TURBULENT FLOW

Robert Blakeley Yule

REPORT

NAVAL POSTGRADUATE SCHOOL

Monterey, California

THESIS

A LASER VELOCIMETER

TO STUDY TURBULENT FLOW

by

Robert Blakeley Yule

December 1974

Thesis Advisor: K. E. Woehler

REPORT DOCUMENTATION PAGE

READ INSTRUCTIONS BEFORE COMPLETING FORM

1. REPORT NUMBER	2. GOVT ACCESSION NO. / 3. RECIPIENT'S CATALOG NUMBER
4. TITLE (and Subtitle): A Laser Velocimeter to Study Turbulent Flow	5. TYPE OF REPORT & PERIOD COVERED: Master's Thesis; December 1974
	6. PERFORMING ORG. REPORT NUMBER
7. AUTHOR(s): Robert Blakeley Yule	8. CONTRACT OR GRANT NUMBER(s)
9. PERFORMING ORGANIZATION NAME AND ADDRESS: Naval Postgraduate School, Monterey, California 93940	10. PROGRAM ELEMENT, PROJECT, TASK AREA & WORK UNIT NUMBERS
11. CONTROLLING OFFICE NAME AND ADDRESS: Naval Postgraduate School, Monterey, California 93940	12. REPORT DATE: December 1974
	13. NUMBER OF PAGES: 70
14. MONITORING AGENCY NAME & ADDRESS (if different from Controlling Office): Naval Postgraduate School, Monterey, California 93940	15. SECURITY CLASS. (of this report): Unclassified
	15a. DECLASSIFICATION/DOWNGRADING SCHEDULE

16. DISTRIBUTION STATEMENT (of this Report)

Approved for public release; distribution unlimited.

17. DISTRIBUTION STATEMENT (of the abstract entered in Block 20, if different from Report)

18. SUPPLEMENTARY NOTES

19. KEY WORDS (Continue on reverse side if necessary and identify by block number)

Laser velocimeter
Laser anemometer
Fluid flow
Turbulent flow

20. ABSTRACT (Continue on reverse side if necessary and identify by block number)

A simple, functional laser velocimeter system for the measurement of fluid flow was designed and constructed. The system was used in a dual scatter, individual realization mode to measure longitudinal velocity components associated with turbulent water flow at low velocity in a transparent tunnel of rectangular cross section. A technique for determining flow characteristics which is independent of the number of

light-scattering particles within the observation volume of the fluid at any one time was developed.

A Laser Velocimeter

to Study Turbulent Flow

by

Robert Blakeley Yule
Lieutenant Commander, United States Navy
B.S., United States Naval Academy, 1964

Submitted in partial fulfillment of the
requirements for the degree of

MASTER OF SCIENCE IN ENGINEERING ACOUSTICS

from the

NAVAL POSTGRADUATE SCHOOL
December 1974

ABSTRACT

A simple, functional laser velocimeter system for the measurement of fluid flow was designed and constructed. The system was used in a dual scatter, individual realization mode to measure longitudinal velocity components associated with turublent water flow at low velocity in a transparent tunnel of rectangular cross section. A technique for determining flow characteristics which is independent of the number of light-scattering particles within the observation volume of the fluid at any one time was developed.

TABLE OF CONTENTS

I. INTRODUCTION - 6

II. EXPERIMENTAL ARRANGEMENT - - - - - - - - - - - - - -11

A. WATER TUNNEL - - - - - - - - - - - - - - - - - -11

B. LASER VELOCIMETER- - - - - - - - - - - - - - - -16

C. INSTRUMENTATION- - - - - - - - - - - - - - - - -25

1. Theory -25

2. Description- - - - - - - - - - - - - - - - - -29

III. SOME TEST MEASUREMENTS AND THEIR RESULTS - - - - -34

A. TEST PROCEDURES- - - - - - - - - - - - - - - - -34

B. PRESENTATION OF DATA - - - - - - - - - - - - - -36

C. DISCUSSION OF RESULTS- - - - - - - - - - - - - -37

IV. SUMMARY AND CONCLUSIONS- - - - - - - - - - - - - -52

APPENDIX A - THE FLOW SYSTEM - - - - - - - - - - - - - -55

APPENDIX B - THE LASER VELOCIMETER SYSTEM- - - - - - - -60

APPENDIX C - EXPERIMENTAL PROCEDURES - - - - - - - - - -63

LIST OF REFERENCES - - - - - - - - - - - - - - - - - - -66

INITIAL DISTRIBUTION LIST- - - - - - - - - - - - - - - -68

I. INTRODUCTION

A laser velocimeter is a device for measuring the local velocity of a substance, usually a moving fluid, by observing the frequency of modulation of scattered laser radiation from the movement of small particles through an interference pattern in the medium. Light from a single laser source is split into two beams which are directed back together in the region of the fluid to be measured. As the two beams cross they form a pattern of high and low intensity (Figure 1) and as particles in the fluid cross this fringe pattern they scatter light which can be detected by a photomultiplier or other light-sensitive device. This variation in light intensity has been shown by Rudd [Ref. 1] to be at a frequency directly proportional to the rate at which particles are crossing the fringe pattern:

$$f = \frac{2\, n\, v\, \sin\theta/2}{\lambda_o} \qquad (1)$$

where n is the refractive index of the medium, v is the velocity component in the plane of the beams perpendicular to a line bisecting the angle between the beams, λ_o is the wavelength of the laser radiation in air, and θ is the angle at which the two beams cross.

The primary advantage of the laser velocimeter over other fluid flow measurement devices, such as the hot-wire

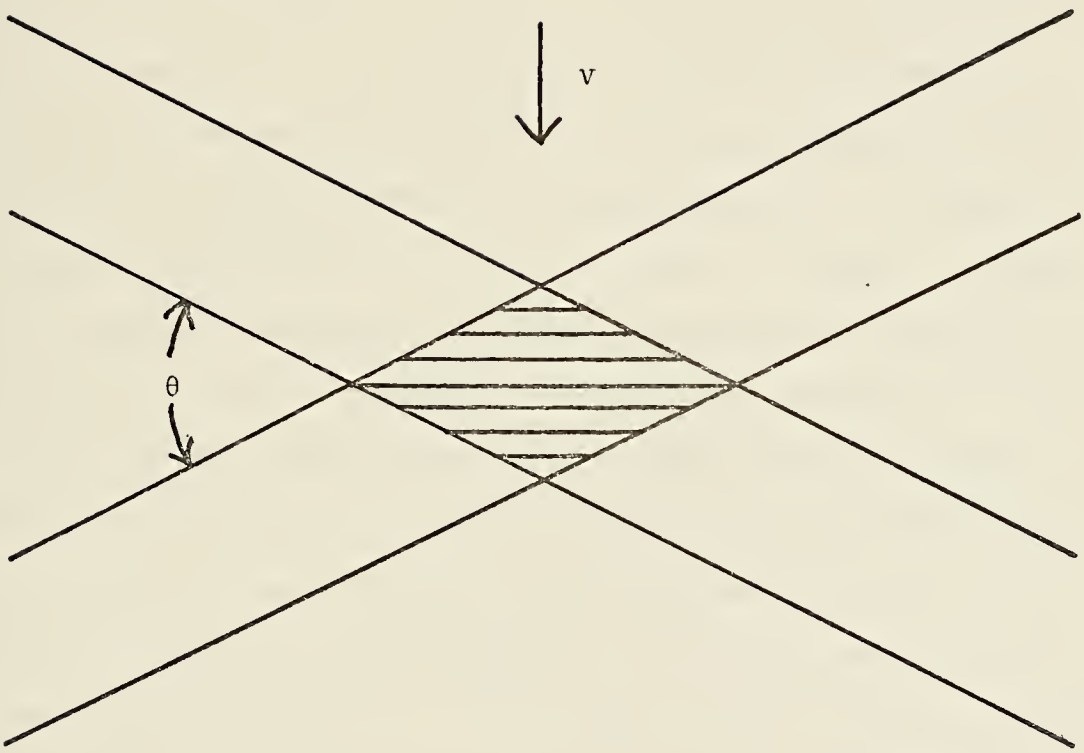

Figure 1. Intensity Pattern of Laser Velocimeter.

anemometer, is that it does not perturb the flow. Furthermore, its small probe volume enables fluid flow to be described in greater detail. Other advantages are the linear response, the lack of calibration requirements, and the directionality of its response.

The first laser velocimeter was constructed by Yeh and Cummins in 1964 [Ref. 2] to measure pipe flow. In 1966 Forman, et al., [Ref. 3] built the first practical instrument, in which a signal beam of scattered light and a reference beam of unscattered light were combined and the resulting scatter detected by a photomultiplier. This system proved difficult to keep aligned, however. In 1969 Rudd [Ref. 4] designed a self-aligning system in which light from a laser was diverged, split into two beams by a two-slit mask, and then focused at a point within the fluid. The scattered light was then focused onto a photomultiplier tube. This system, known as the dual scatter system, was easier to align and also improved the signal-to-noise ratio at the photomultiplier. It is this system, with minor variations, that has since been used by most investigators.

Information on turbulence in a fluid flow can be derived with a laser velocimeter by spectrum analysis of a basically continuous signal from the photomultiplier. If necessary to achieve a relatively continuous signal, the flow is seeded with small particles so that there are always enough scatters within the probe volume to yield a sufficient signal-to-noise ratio. This method has been used by numerous

investigators [Refs. 5, 6, and 7] to measure the mean flow velocity, rms fluctuation velocity, and the velocity probability density function of turbulent flows. There are two serious disadvantages associated with continuous signal laser velocimeter measurements of turbulence. First, the signal can either fade if the number of scattering particles is too low, or it can saturate the photomultiplier if the number of scattering particles is too high. Second, a fundamental ambiguity due primarily to the finite travel time of particles through the scattering volume causes a broadening of the frequency spectra which is not associated with the turbulence of the flow.

To overcome these disadvantages, Donohue, et al., [Ref. 8] designed a system which utilized a non-continuous signal to measure the velocity of individual scatterers within the volume enclosed by the two crossing laser beams. The number of scattering particles was kept low enough so that there was at most one particle in the scattering volume at any one time. As each particle crossed the volume it scattered a burst of light onto the photomultiplier. Individual velocity realizations at a point in space were then recorded in a histogram from which mean velocity and other properties of turbulence could be interpreted. A difficulty with this method is that either the rate at which particles cross the observation volume must be kept constant during the measurement of a velocity provile, or,

when such control is not possible, the data taking and processing must account for possible variations of the scattering particle number.

The purpose of the study which is presented here was to build from easily available components a working laser velocimeter which uses individual realizations but automatically sorts the results into speed bins. In order to ensure individual realizations a low-speed water tunnel was constructed. Since the emphasis was on building a workable velocimeter for future studies of turbulent wakes in drag-reducing fluids, no particular precautions regarding the flow were taken at this time and the flow was expected to be turbulent. Some measurements at a mean flow velocity corresponding to a Reynolds Number of 45 were made. The relative rate of occurrence of a specific frequency in the scattered light signal, corresponding to a particular velocity within the fluid, was determined. From data collected during measured intervals of time, and at different frequencies, a velocity probability density function was constructed from which various properties of turublence could be derived.

II. EXPERIMENTAL ARRANGEMENT

The experiment consisted of designing, building, and testing a laser velocimeter and water tunnel for the purpose of studying different conditions of fluid flow. The design was based on a desire, in future experiments, to inquire into the properties of wakes behind submerged bodies of different configuration, and into the effect of drag-reducing agents on such wakes. This ultimate objective governed the overall shape and size of the water tunnel. It had to be large enough to preclude wall effects from disturbing the wake generated behind a body positioned on the longitudinal flow axis. The size of the tunnel, then, coupled with limited available pressure head, dictated that the experiment be performed at low fluid flow velocities.

The following is a qualitative discussion of the system design parameters. A more detailed description of the system components and experimental procedures is contained in the appendices.

A. WATER TUNNEL

The first consideration in the design of the water tunnel was the size of the cross sectional area. It had to be large enough so that wall effects would not distort the wake behind the test body. An order of magnitude estimation was made based on the discussion of the two-dimensional wake behind a single body by Schlichting

[Ref. 9]. This type of wake is formed, for example, behind a circular cylinder placed normal to the flow axis (Figure 2). The wake is described by the equation:

$$b = 0.18 \sqrt{10} \, (xC_d d)^{1/2} \qquad (2)$$

where b is the half-width of the wake at a distance x behind the body, C_d is the drag coefficient, and d is the diameter of the cylinder. Measurements by Schlichting [Ref. 9] have confirmed that the wake width is related to the Prandtl mixing length, l, as follows:

$$l/b = 0.18 \, . \qquad (3)$$

Given a 0.1 cm width of the laser beam crossing region, it should be possible to study turbulent fields with mixing lengths down to 0.4 cm. (The 0.1 cm probe can still discern some structure inside one mixing length.) From equation (3) the desired half-width of the wake for this resolution and mixing length would be 2.2 cm, and the total width of the wake at the selected point of measurement, 2b, would be 1.73 in. In order to minimize the chance of wall effects interfering with the wake, a tunnel lateral dimension of 6 in. was chosen.

To determine an appropriate length for the tunnel, equation (2) was used, in which b = 2.2 cm, C_d = 0.74 [Ref. 10], and d = 1.0 cm, to yield x = 20.6 cm = 8.2 in. Thus, for the required spatial resolution the probe should

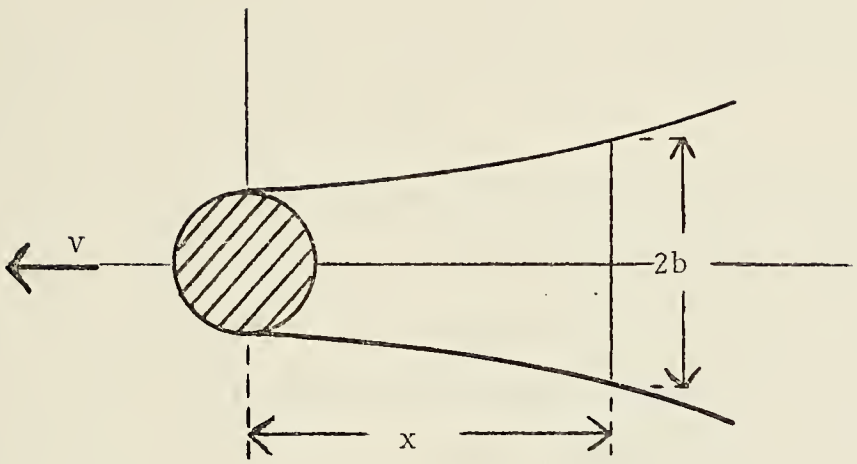

Figure 2. Wake behind Circular Cylinder Placed Normal to Flow Axis.

be placed 8.2 in. behind the body. An overall length of 48 in. was chosen in order to try to ensure that the flow would have become essentially laminar by the time it reached the vicinity of the body placed midway down the tunnel.

A slight disadvantage of the laser velocimeter is that the beams must enter the flow volume through a plane transparent surface in order to avoid spherical aberration and consequent loss of scattered light signal. This necessitated that the tunnel have a rectangular cross section. Some secondary flow was therefore expected but it was not thought to be significant because of the large cross sectional area of the tunnel.

The result of the preceding considerations was the 48 in. x 6 in. x 6 in. Lucite water tunnel shown in Figure 3. The inlet region of the tunnel proved to be a significant source of undesirable turbulence because of the sudden transition of the flow from a circular inlet pipe to a square tunnel. A smooth transition of cross sectional areas from circular to square could only be approximated by the adaptor shown in Figure 3. Caulking compound was used to fill in the corners of the adaptor, but this had only a marginal effect on the degree of turbulence at the inlet of the tunnel. The problem of removing the channel turbulence was left unsolved. For testing of the velocimeter, the channel turbulence would serve as an equally suitable object.

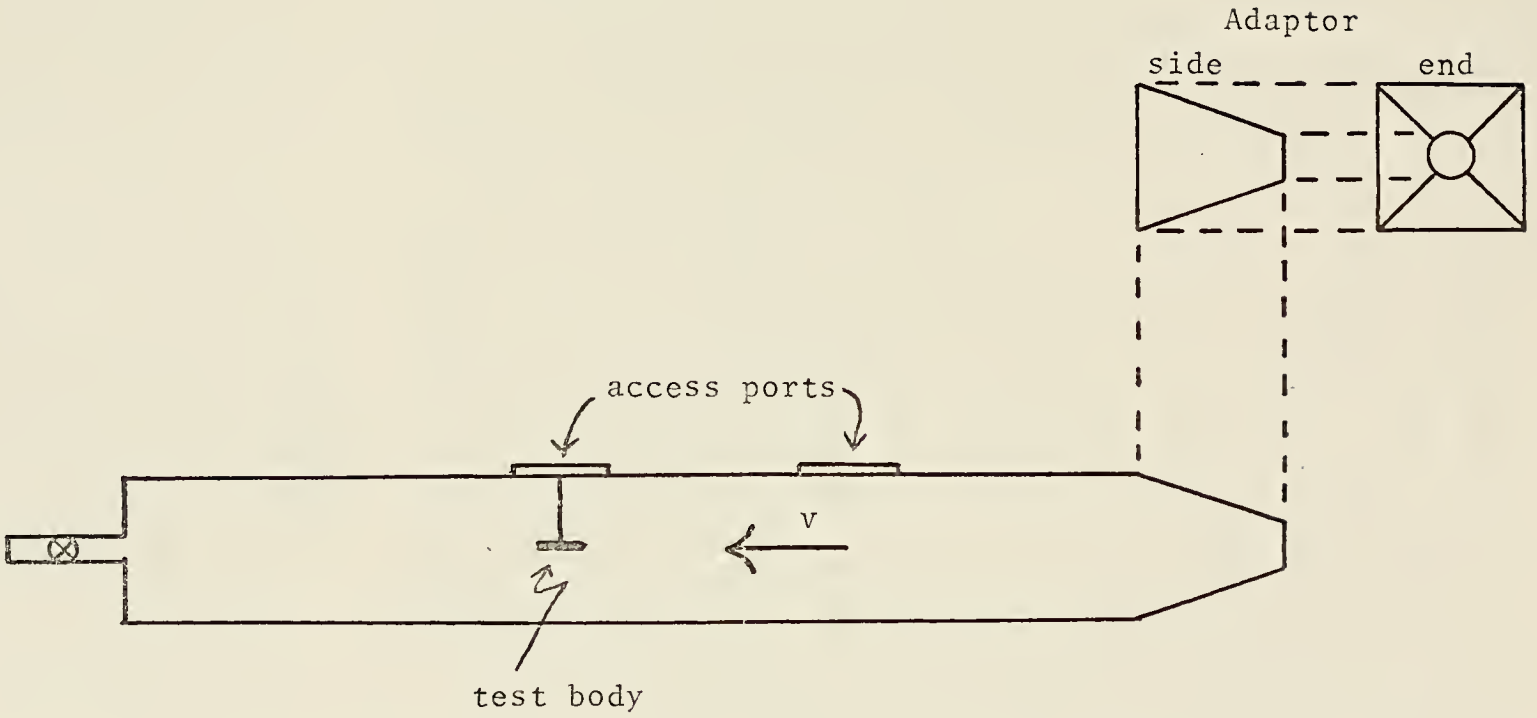

Figure 3. Water Tunnel

B. LASER VELOCIMETER

Since the laser velocimeter was first used by Yeh and Cummins in 1964 [Ref. 2], several theories describing its operation have been suggested. They may all be grouped into two models, however. In one first described by Goldstein and Kreid in 1967 [Ref. 11], the light scattered by a particle crossing a single monochromatic beam of radiation is Doppler-shifted due to the motion of the particle. Alternatively, Rudd [Ref. 1] has described an equivalent model which is easier to visualize and has been preferred by most investigators. In the Rudd model, two mutually coherent beams of monochromatic radiation are made to cross within a flow medium. Within the volume where the beams cross, an interference pattern of regions of high and low intensity, i.e., a fringe pattern, is formed as shown in Figure 4. The fringes are parallel to the bisector of θ, the angle between the two beams. The spacing between the fringes in a medium of refractive index n is given by:

$$d = \frac{\lambda_o}{2\ n\ \sin\theta/2} \tag{4}$$

in which λ_o is the wave length of the light source in air. If a particle crosses the pattern with a velocity component v, normal to the fringes, the scattered light as it passes through the regions of the high and low intensity will fluctuate at a frequency described by:

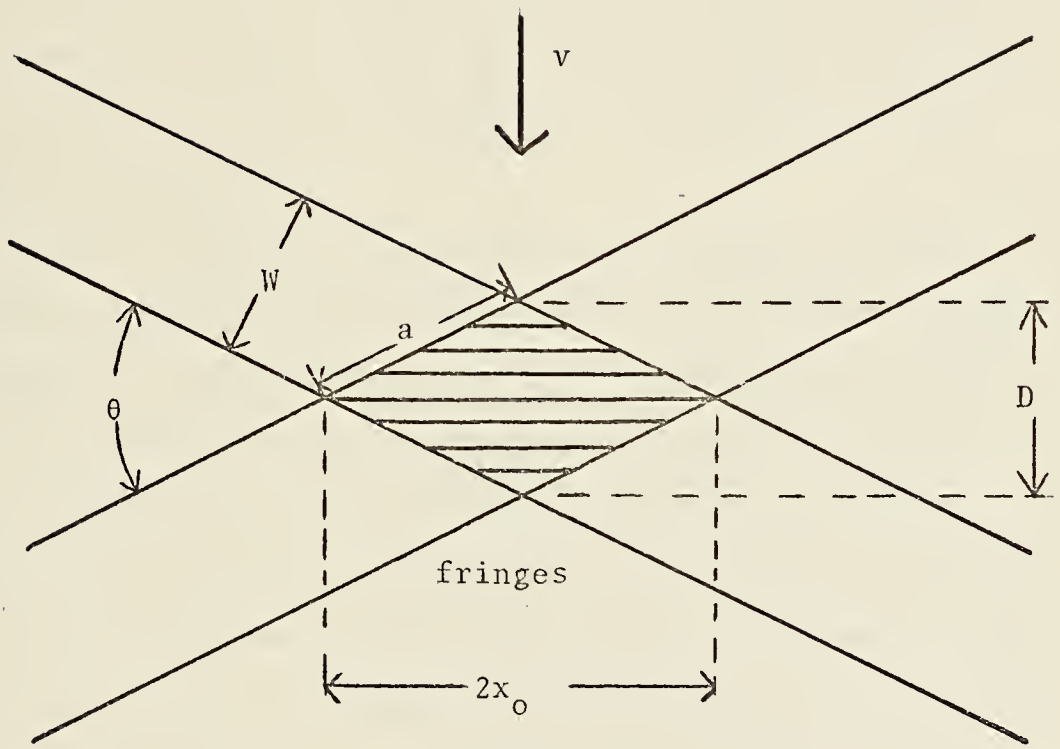

Figure 4. Geometry of Beam Crossing Region of Laser Velocimeter.

$$f = \frac{v}{d} = \frac{2\ n\ v\ \sin\theta/2}{\lambda_o} \quad . \tag{5}$$

Therefore, the frequency of the scattered light is directly proportional to the component of particle velocity normal to the fringes. If the particle is small enough to follow the motion of the medium, the frequency of light fluctuations accurately represents the character of the flow. The scattered light can be focused onto a photo-detection device which produces a signal at the frequency of the light fluctuations.

After a survey of the available literature it was decided that the "dual scatter" laser velocimeter system designed by Rudd [Ref. 4], with minor variations, would be best suited for the measurement of turbulence in the water tunnel since it seemed to be relatively easy to align (and to keep in alignment) and it offered a higher signal-to-noise ratio than other systems. Because of the low fluid velocity within the water tunnel, it was thought that the individual realization method of Donohue, et al., [Ref. 8], whereby a non-continuous scattered light signal is used to measure the velocities of the individual scatterers within the probe volume, would be most appropriate for this experiment.

The optical arrangement of the laser velocimeter used in this experiment is shown in Figure 5. The single beam of light from the laser is split into two diverging beams

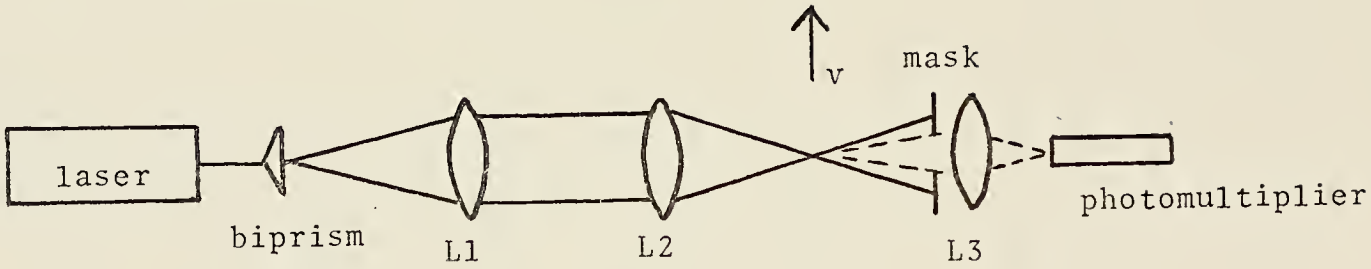

Figure 5. Laser Velocimeter Optical Arrangement.

of equal intensity which are made parallel by lens L1, then focused by lens L2 so as to cross within the flow. After leaving the flow area, the two beams are blocked by a mask so that only forward scattered radiation is focused by lens L3 onto the photomultiplier tube.

This laser velocimeter was designed, constructed, and employed relying on information gained from the literature available up to the time of the experiment. In a more recent paper by Hill [Ref. 12] on the geometric parameters of a laser velocimeter, an argument is presented for describing the intensity pattern of the crossing volume by means of Fourier optics whereby the geometry of the fringe pattern of the crossing beams is related to the geometry of the optics of the velocimeter. The form of the voltage signal from the photo-detection device is directly related to the form of the fringe pattern.

An attempt is made here to relate the geometry of the laser velocimeter used in this experiment to Hill's criteria with a view toward achieving a better understanding of the results of some test measurements made with the system. The parameters of the system are as follows:

λ_o = wave length in air of the He-Ne laser used in this experiment

= 6.328×10^{-5} cm

v = mean velocity of fluid (as derived from actual flow rate measurement)

= 0.72 cm/sec

n = refractive index of the medium

= 1.33 for water.

h = separation distance between the two beams at lens L2 (see Figure 6)

= 0.9 cm

1 = focal length of lens L2 (also, = distance between lens L2 and the beam crossing point)

= 10.0 cm

θ = beam crossing angle

= 5.1°

W = diameter of individual beam, measured at the lens

= 0.1 cm

Using these parameters, the dimensions of the beam crossing region are calculated as follows:

1. Fringe Spacing

From Rudd [Ref. 1] the distance between adjacent fringes is:

$$d = \frac{\lambda_o}{2\ n\ \sin\theta/2} \qquad (6)$$

$$= 5.3 \times 10^{-4} \text{ cm } (= 5.3 \text{ microns})$$

2. Number of Fringes in Pattern

Referring to Figure 4, for small crossing angles the width of the pattern, D, is approximately equal to the width of a beam, W. Then, the number of fringes expected within the pattern is:

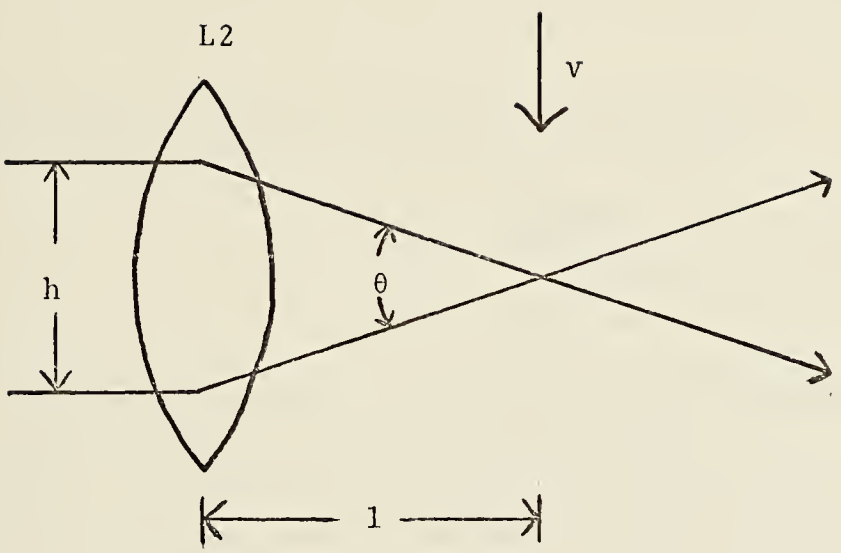

Figure 6. Geometry of Laser Velocimeter Optics.

$$K = D/d$$

$$k = 186 \text{ fringes.} \tag{7}$$

3. Spatial Resolution

Referring to Figure 4, the spatial resolution may be expressed as the maximum lateral dimension of the region, $2x_o$. Using the following relationships:

$$\sin \theta = W/a \tag{8}$$

$$\cos \theta = x_o/a \tag{9}$$

the spatial resolution may be expressed as:

$$2x_o = \frac{2W\cos\theta/2}{\sin \theta}$$

$$2x_o = 2.22 \text{ cm} . \tag{10}$$

Some observations pertaining to the dimensions of the intensity pattern are offered at this point. First, the fringe spacing distance dictates that, optimally, scatter particles be of a size no larger than 5.3 microns so that the resulting signal would truly represent the particle's velocity.

Second, the number of fringes calculated above was not supported by actual observation. Oscilloscope traces of the signal indicated that fewer fringes were being crossed within the region. Hill's criteria predicted that for the given geometry, the number of fringes within the volume would be 22. This figure correlated well with visual

observation and was therefore thought to better describe the actual number present. Proceeding then under the assumption that 22 fringes were present in the pattern, from equation (7), the effective width of the intensity pattern, and therefore the beam width, was only 0.01 cm. This apparent power of ten reduction in the width of an individual beam from the lens to the crossing region could be explained by an actual focusing by the lens of the light within the beam, or it may be due to a lack of coherence of the outer portions of the beam in the crossing region which would reduce the effective number of fringes. This discrepancy is not resolved at this time.

Third, the calculated spatial resolution of 2.22 cm is too large for a meaningful velocity measurement to be made in a wake of the size to be found in the present tunnel. An optimum beam crossing angle of $\theta = 90°$ would yield a spatial resolution of 0.24 cm which would make wake measurements in the tunnel meaningful; however, widening the crossing angle would call for a more complicated optical arrangement, usually requiring mirrors, and a consequent increase in the size of the laser velocimeter unit. An additional benefit, though, is that the mean frequency would be higher, thus facilitating spectrum analysis since the spectrum of the flow would be further removed from the high amplitude, low frequency components. If the effective width of a beam was indeed reduced by ten, as it appeared

in this experiment, then a corresponding spatial resolution of 0.22 cm would have provided meaningful results. Additional investigation into the actual effective size of the beam crossing is required.

C. INSTRUMENTATION

1. Theory

Several methods for converting the scattered light signal from a laser velocimeter into velocity information have been proposed and utilized with varying degrees of success. These include the use of spectrum analyzers, tracking filters, discriminators, and correlators. Of these signal processing systems, the simplest and most widely used to date has been the spectrum analyzer. Because of its simplicity and wide availability, the spectrum analyzer was chosen as the basis for the signal processing used in this experiment. A counting scheme was employed to measure the relative strength of different frequencies present in the scattered light.

In his paper Hill estimated the frequency spectrum due to the photomultiplier signal from a single particle realization. The signal is expected to be of the form shown in Figure 7.

The primary frequency contained in v(t) is $f_o = \frac{v}{d}$ where d is the fringe distance and v the particle velocity. The modulation is caused by the laser beam's intensity profile.

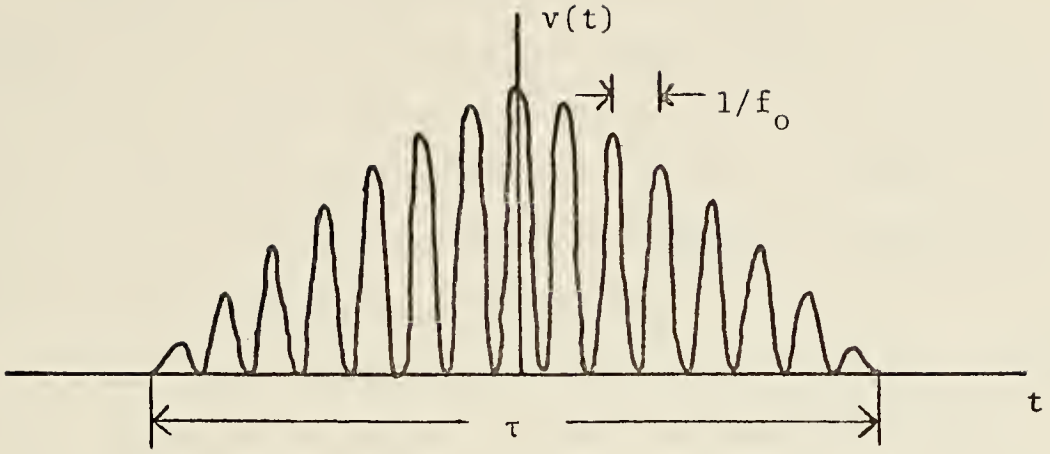

Figure 7. Laser Velocimeter Signal due to Single Particle.

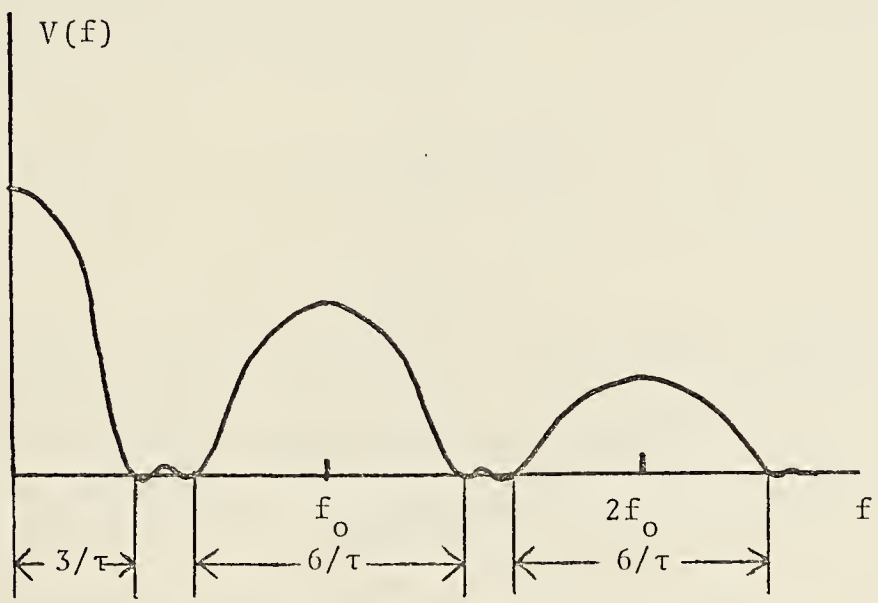

Figure 8. Fourier Spectrum of Laser Velocimeter Signal due to One Particle.

Figure 8 shows the Fourier spectrum of v(t) as derived by Hill. If the scattered light intensity varies as $\cos^2 2\pi f_o t$ as Hill seems to suggest, it is not clear why f_o is in the spectrum (since $\cos^2\theta = 1/2 + 1/2 \cos 2\theta$). It is not clear at this point what the frequency content of the individual realizations should be.

The pulse length, τ, of v(t) is the time for a single particle to cross the probe region. The maximum τ for a particle moving at mean velocity is:

$$\tau = \frac{2.44\lambda_o 1}{nWv} \qquad (11)$$

$$= 16.1 \text{ msec for this experiment.}$$

The expected mean frequency, f_o, for a mean flow velocity of 0.72 cm/sec is, from equation (5):

$$f_o = \frac{2nv \sin\theta/2}{\lambda_o} \qquad (5a)$$

$$= 1362 \text{ Hz.}$$

From Figure (8) it can be seen that for good frequency resolution two criteria are necessary:

(1) $f_o >> \frac{3}{\tau}$

(2) τ as large as possible.

Figure (9) demonstrates that, for a given mean flow velocity, beam diameter, and lens focal length, the pulse

Note: $\tau = \frac{D}{V}$

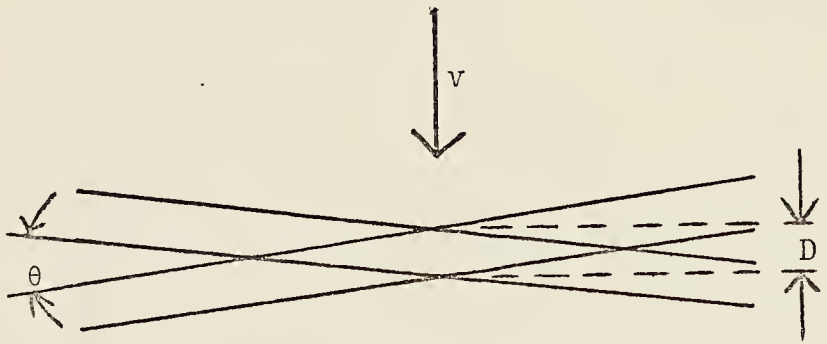

(a) Small θ → large $2x_o$ → small τ

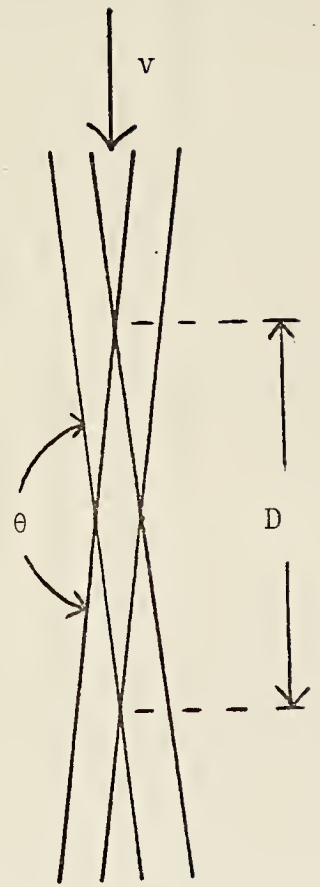

(b) Large θ → small $2x_o$ → large τ

Figure 9. The Effect of Probe Volume Dimension on Frequency Resolution.

length is greater for a narrower probe volume. Therefore, from the frequency resolution aspect, it would also be advantageous to increase the beam crossing angle.

From the expected spectrum for the signal (Figure 10) using the calculated value of τ from equation (11) and the parameters of the system, it can be anticipated that because of the apparently adequate spread between f_o and $\frac{3}{\tau}$, there would be no frequency resolution problem. However, this model does not take into account such factors as ambient noise, actual fluid turbulence, and additional light scatter from particles crossing a beam near ends of the probe volume, all of which would contribute to broadening of the spectrum natural line width about f_o.

2. Description

The scattered light signal from the photomultiplier was fed into an SKL Variable Electronic Filter (Model 302) which was set to reject all frequency components less than 400 Hz and greater than 3000 Hz. This frequency range was selected because the filter rejects the low frequency "envelope" of the signal which is not related to the fluid velocity, and because it covers the range of expected frequencies as calculated from equation (5). After filtering, the signal was fed into a Hewlett-Packard Wave Analyzer (Model 302A) set at a desired frequency. The restored single frequency output of the wave analyzer, the amplitude of which varied with the strength of that

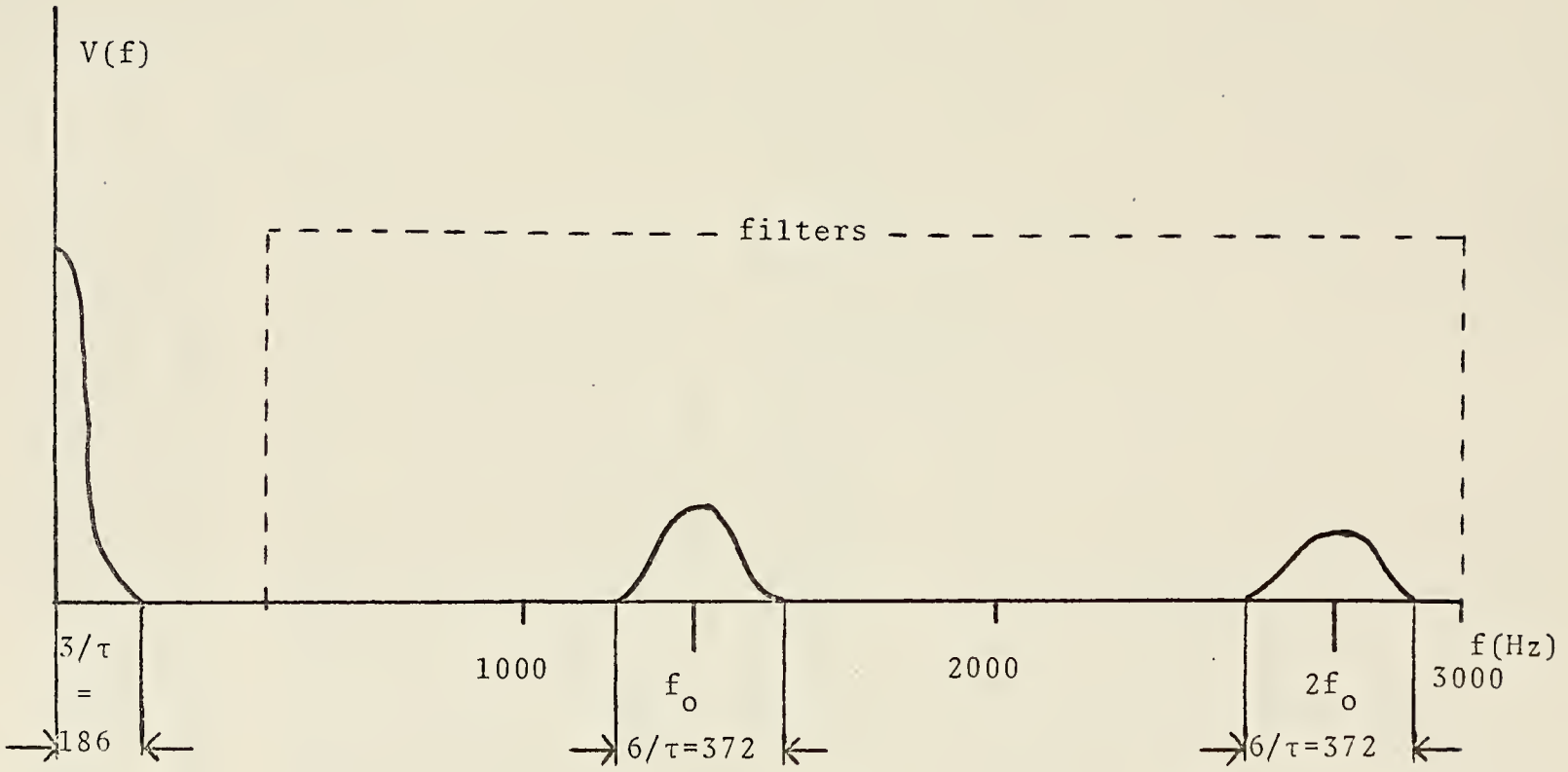

Figure 10. Expected Frequency Spectrum of Laser Velocimeter Signal.

particular frequency component of the input signal, was amplified with a Hewlett-Packard Power Amplifier (Model 467A), and then sent to Tektronix Dual Beam Oscilloscope (Type 565). The trigger level of this oscilloscope was set so that the scope trace triggered only when the input signal exceeded two volts. This value of triggering level was decided upon since it allowed for counting of a sufficient number of excursions above threshold over the whole frequency range. The Tektronix scope in turn triggered a Hewlett-Packard Timer-Scaler (Model 5201 L) which counted the number of times the output of the wave analyzer exceeded threshold within a certain period.

If the signal from the photomultiplier, v(t), had the same form as the intensity pattern of the probe region, as proposed by Hill, then the Timer-Scaler was actually recording the number of fringes crossed by a single particle traveling at the specific velocity corresponding to the frequency at which the wave analyzer was set. In Figure 11, for example, eleven counts would be recorded corresponding to eleven positive excursions of the signal above threshold, for each particle that crossed the probe volume at the velocity under study.

Finally, a Hewlett-Packard Oscilloscope (Model 130 BR) was set to continuously monitor the filtered signal from the photomultiplier. A schematic of this system arrangement is shown in Figure 12.

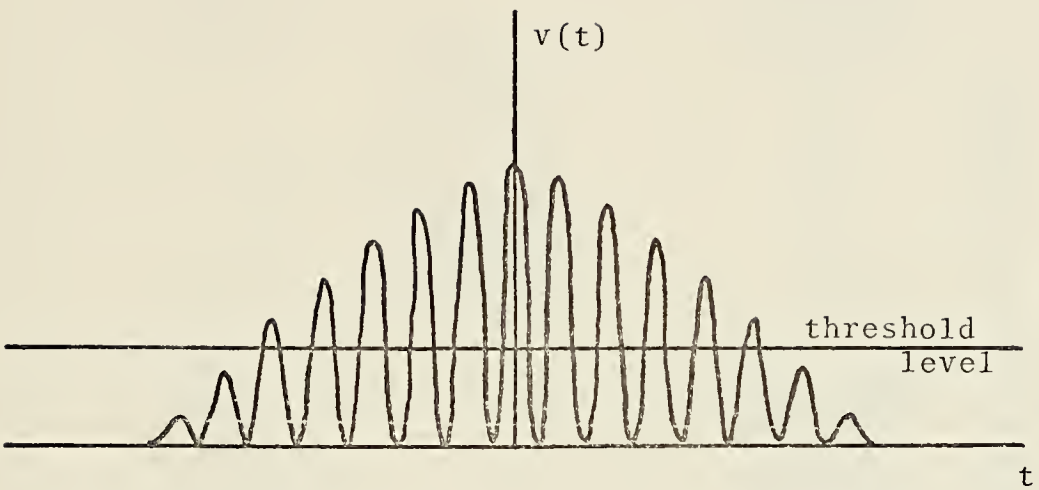

Figure 11. Effect of Threshold Level on Laser Velocimeter Signal.

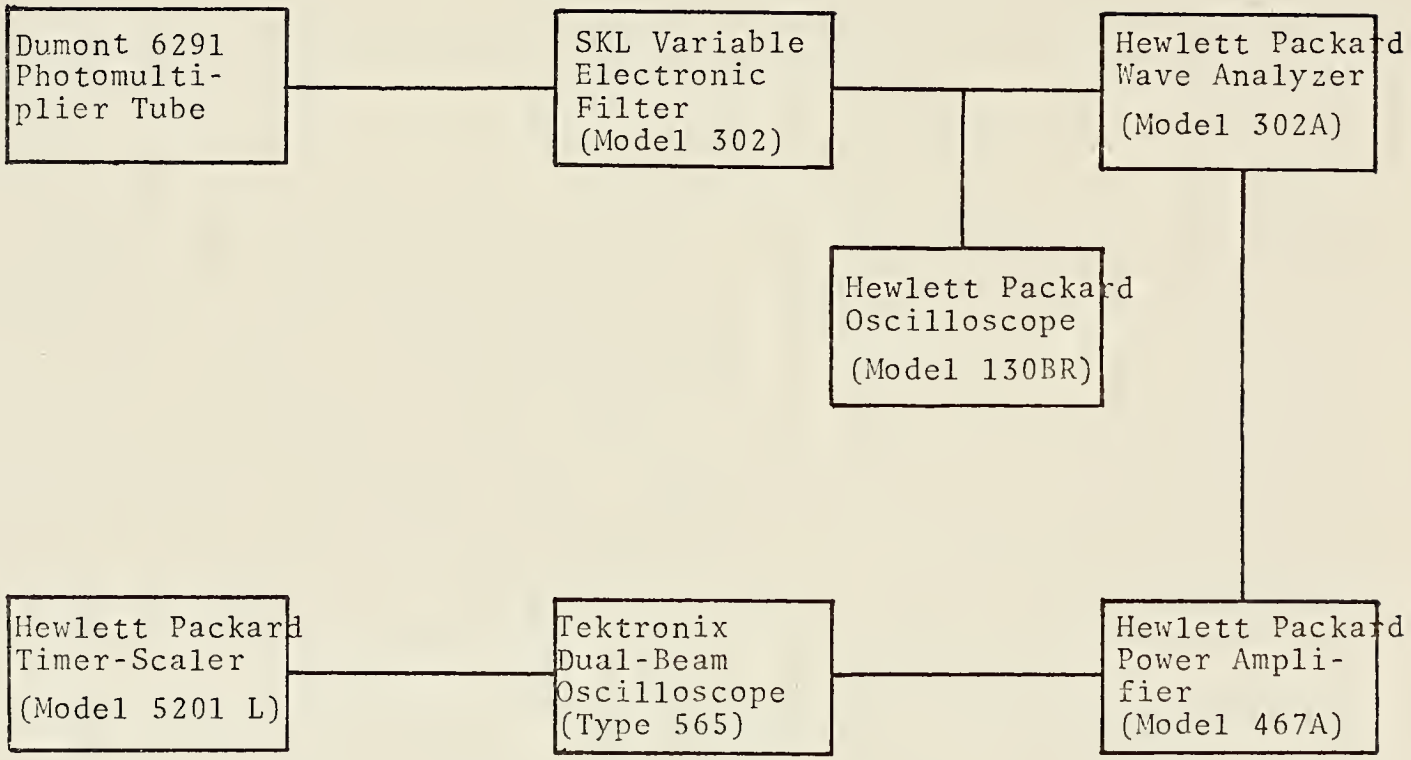

Figure 12. Instrumentation Arrangement.

III. SOME TEST MEASUREMENTS AND THEIR RESULTS

A. TEST PROCEDURES

Measurements were made at two positions within the flow: on the longitudinal centerline of the tunnel, and at a position two-thirds of the distance between the centerline and the side wall of the tunnel. Measurements were taken for two different flow conditions. In one case the flow was unperturbed; in the other case, the probe volume was positioned ten cm downstream from a 1/4 in. diameter right circular cylinder placed perpendicular to the flow axis.

The measurement procedure consisted of setting the wave analyzer at a frequency and then counting the number of times the analyzer output signal exceeded a preset threshold level within one minute periods. Five such threshold crossing totals were recorded for each frequency. Measurements were made at 100 Hz intervals over the frequency range between 400 Hz and 3000 Hz. After each series of five measurements was made at a particular frequency, one measurement was made at a "standard" frequency of 1500 Hz. This measurement was taken to determine if the threshold crossing rate was changing because the fluid velocity corresponding to the frequency setting was occurring a different percentage of time or merely because of changes in particle density within the fluid.

The number of threshold crossings within a specified time interval, when averaged over a number of intervals, gave a statistical indication of the relative occurrance of a particular frequency within the scattered light and therefore of a particular velocity within the flow. From this information, velocity probability density functions were constructed which enabled the turbulence characteristics of the flow to be studied.

The number of recorded threshold crossings within a certain period is related to the number of individual velocity realizations for that period by:

$$N = \frac{T}{K} \tag{12}$$

where N is the number of realizations, T is the number of measured threshold crossings, and K is the number of fringes in the probe volume light intensity pattern. An important factor regarding the construction of a velocity probability density function for turbulent flow is the accuracy of the distribution based on a given number of realizations. If it is assumed that the number of realizations is normally distributed, and that the standard deviation of the realizations is equivalent to the root-mean-square of the velocity fluctuations, then a reasonable estimate of the accuracy with which the mean velocity is measured can be made.

According to Donohue, et al., [Ref. 8], the accuracy with which the true mean of the distribution is measured,

based on the number of realizations, is approximately:

$$\text{Accuracy} = \frac{\Delta\bar{v}}{\bar{v}} = \frac{2(\sigma/\mu)}{\sqrt{N}} \qquad (13)$$

where $\bar{v}$ is the true mean flow velocity, $\Delta\bar{v}$ is the departure of the measured value of mean velocity from the true value, σ is the standard deviation of the distribution, and μ is the mean of the distribution. For an average number of measured threshold crossings required to construct a distribution of 46,000, and assuming an intensity pattern containing 22 fringes, the average number of realizations measured is, from equation (12), 2090. Using this figure in equation (13) and assuming that the flow is fifty per cent turbulent, then it is estimated that, on the average, the resulting velocity probability density functions should be accurate to within 2.2 per cent. There are, however, other error producing influences which will be discussed.

B. PRESENTATION OF DATA

Figures 14 through 23 are the velocity probability density functions for two different conditions of flow at two different positions. In Figures 14 through 17 and Figure 22, the ordinate represents the number of threshold crossings of the analyzer output signal in a one-minute period. In Figures 18 through 21 and Figure 23 the ordinate represents the number of threshold crossings per minute normalized by dividing the values at each frequency by the

number of threshold crossings per minute at 1500 Hz recorded after the five measurements at that frequency. For all profiles the mean number of threshold crossings was obtained by averaging over five one-minute intervals. Error bars of length 2σ were superimposed.

Figures 22 and 23 are for the same position and flow conditions as Figures 16 and 20, and were made to see whether the possible discontinuity of Figure 16 in the vicinity of 2200 Hz is real. Efforts to study this area more closely resulted in the profiles in Figures 22 and 23.

C. DISCUSSION OF RESULTS

All profiles evidence, to some extent, a Gaussian-like distribution expected with turbulent flow. The unnormalized profiles show a peak in the vicinity of 900-1000 Hz which is somewhat lower than the f_o of 1362 Hz predicted by equation (5). This frequency difference corresponds to a mean velocity shortfall of some 0.22 cm/sec which may have been due to a counter-flow set up by the abrupt termination of the tunnel.

In all profiles the frequency spread is much greater than the $6/\tau$ value of 372 Hz predicted as the "natural width." The additional frequency broadening then can be attributed to the turbulent nature of the flow. However, some broadening may also be caused by ambient noise as well as by scatter from particles crossing a light beam outside of the probe volume. There is some indication of a

secondary maximum around 2000 Hz, as predicted by the expected spectrum of the photomultiplier signal but again it is much broader than the 372 Hz.

In all profiles the left side of the distribution usually associated with turbulence is absent because of a preponderance of low frequency components. These strong low frequency contributions may be caused by particles passing through the probe volume which are larger than the distance between adjacent fringes of the intensity pattern (5.3 microns). In future experiments of this type care should be taken to filter out such particles.

Since the method of measuring individual velocity realizations is based on a constant particle flux density in the observation region, a normalization scheme was employed to account for changes in particle density. The normalized curves included here have the same general features as the unnormalized curves, but to a lesser degree. In particular the difference in slopes for different flow conditions, so pronounded in the unnormalized curves, is less evident.

Any interpretation of the profiles obtained here must be viewed with great reservation at this point since the standard frequency measurement was recorded only once for every five measurements at a particular frequency. It is believed that a proper normalization procedure requires simultaneous measurements at the standard frequency and at the frequency under observation. By means of a parallel

wave analyzer-oscilloscope-counter combination the number of threshold crossings per minute for a standard frequency could be recorded at the same time as the number of crossings for each frequency observed. In this way the effects of instantaneous changes in particle density could be eliminated.

The profiles show significant scattering of the threshold crossing rate data, especially at higher frequencies. This variation, while large, is not unexpected when consideration is given to the geometry of the probe volume (see Figure 13).

If it is assumed that a particle within the probe volume is equally likely to cross the intensity pattern at any value of x, and that the number of fringes crossed by a particle is equally likely to be any number between 0 and 22 (the total number of fringes), then the standard deviation, σ_K, of the expected number of fringes crossed by a single particle is found to be 6.35. The mean value of the number of fringes crossed, μ_K, is calculated to be 11. Thus $(\frac{\sigma}{\mu})_K = 57.7\%$. This is of the same order of magnitude as, though somewhat larger than, the average $\frac{\sigma}{\mu}$ for all five unnormalized curves, which is 26.7%. Thus it can be postulated that the wide variability in the data may be due to the fact that not all particles in the observation region crossed all 22 fringes of the intensity pattern.

It is difficult to derive a true characterization of flow turbulence from the profiles presented here because of

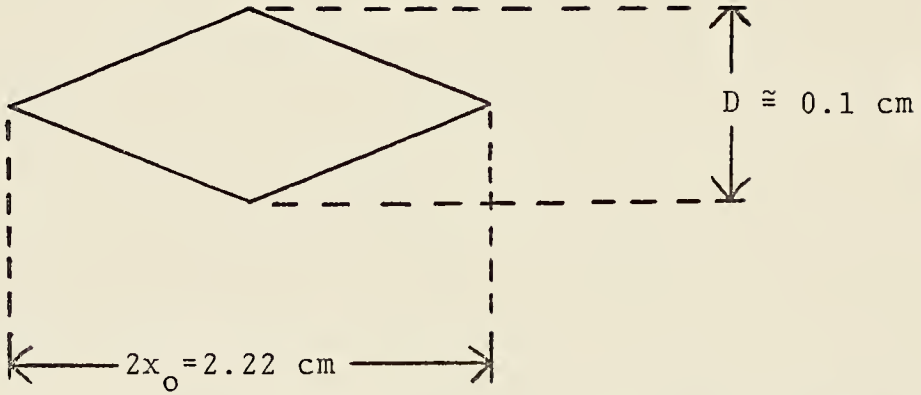

Figure 13. Geometry of Probe Volume.

the presence of other factors not related to the flow which influence the shapes of the profiles. The effects of these factors must be firmly quantified in future experiments of this kind if the data obtained are to be meaningful.

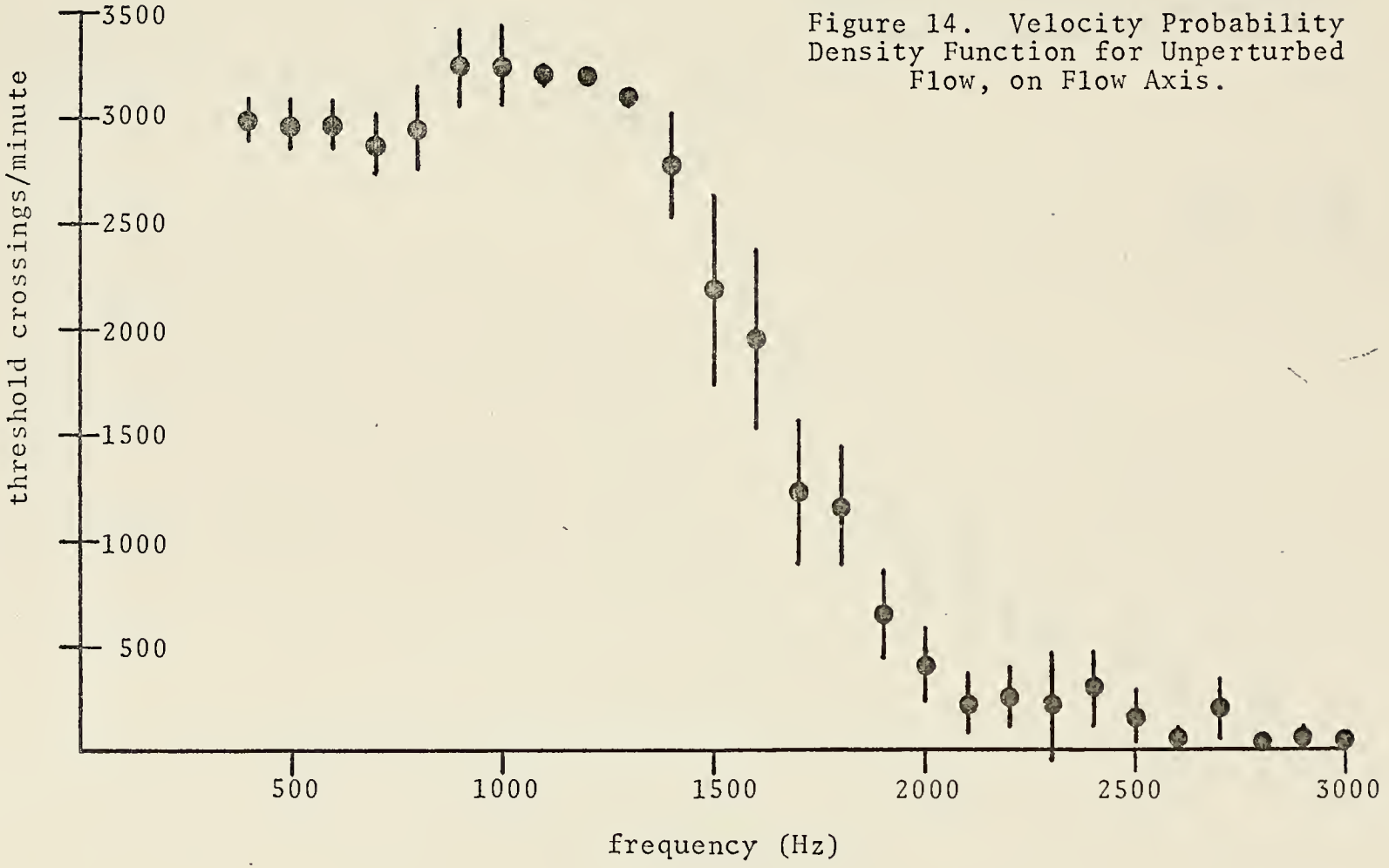

Figure 14. Velocity Probability Density Function for Unperturbed Flow, on Flow Axis.

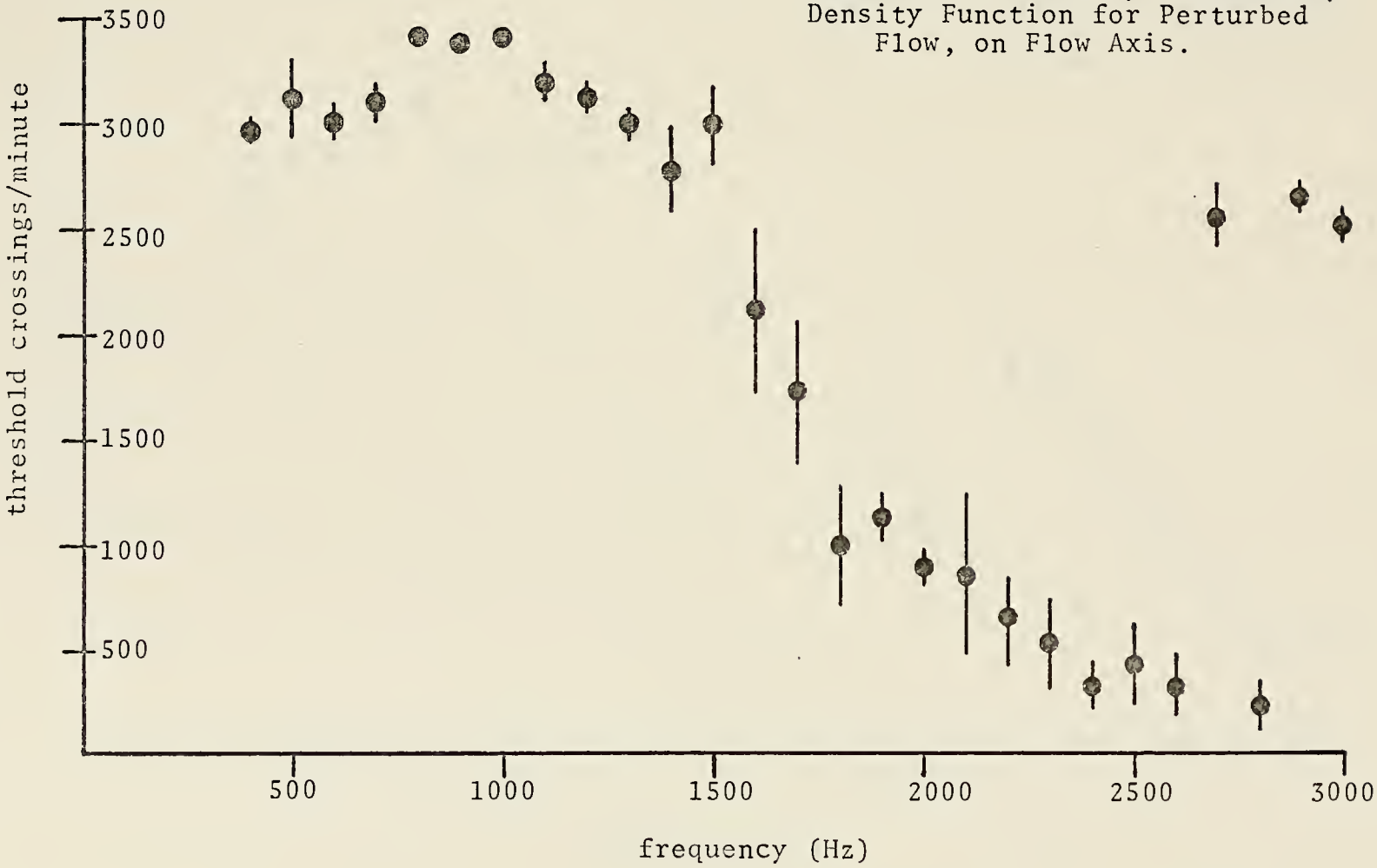

Figure 15. Velocity Probability Density Function for Perturbed Flow, on Flow Axis.

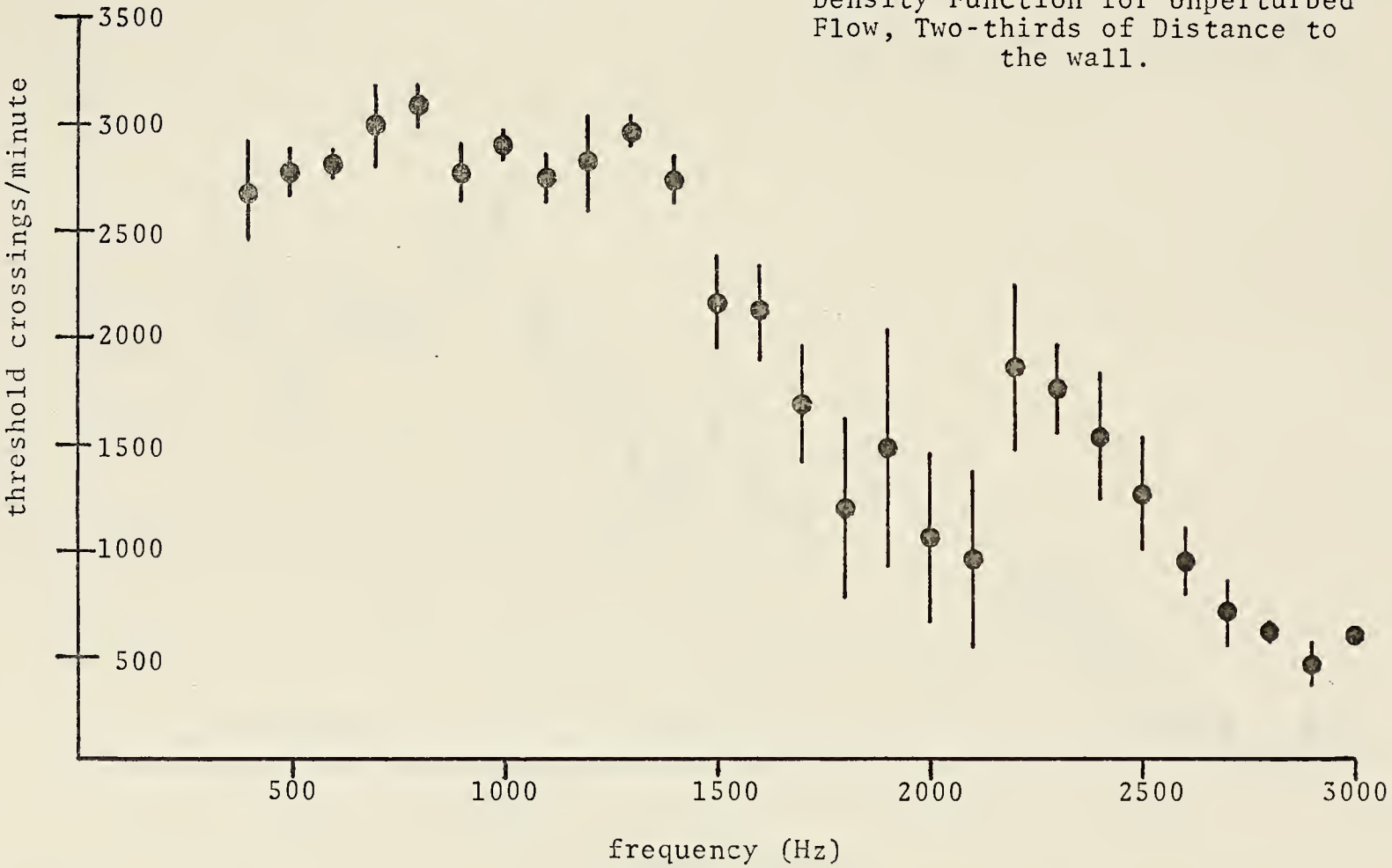

Figure 16. Velocity Probability Density Function for Unperturbed Flow, Two-thirds of Distance to the wall.

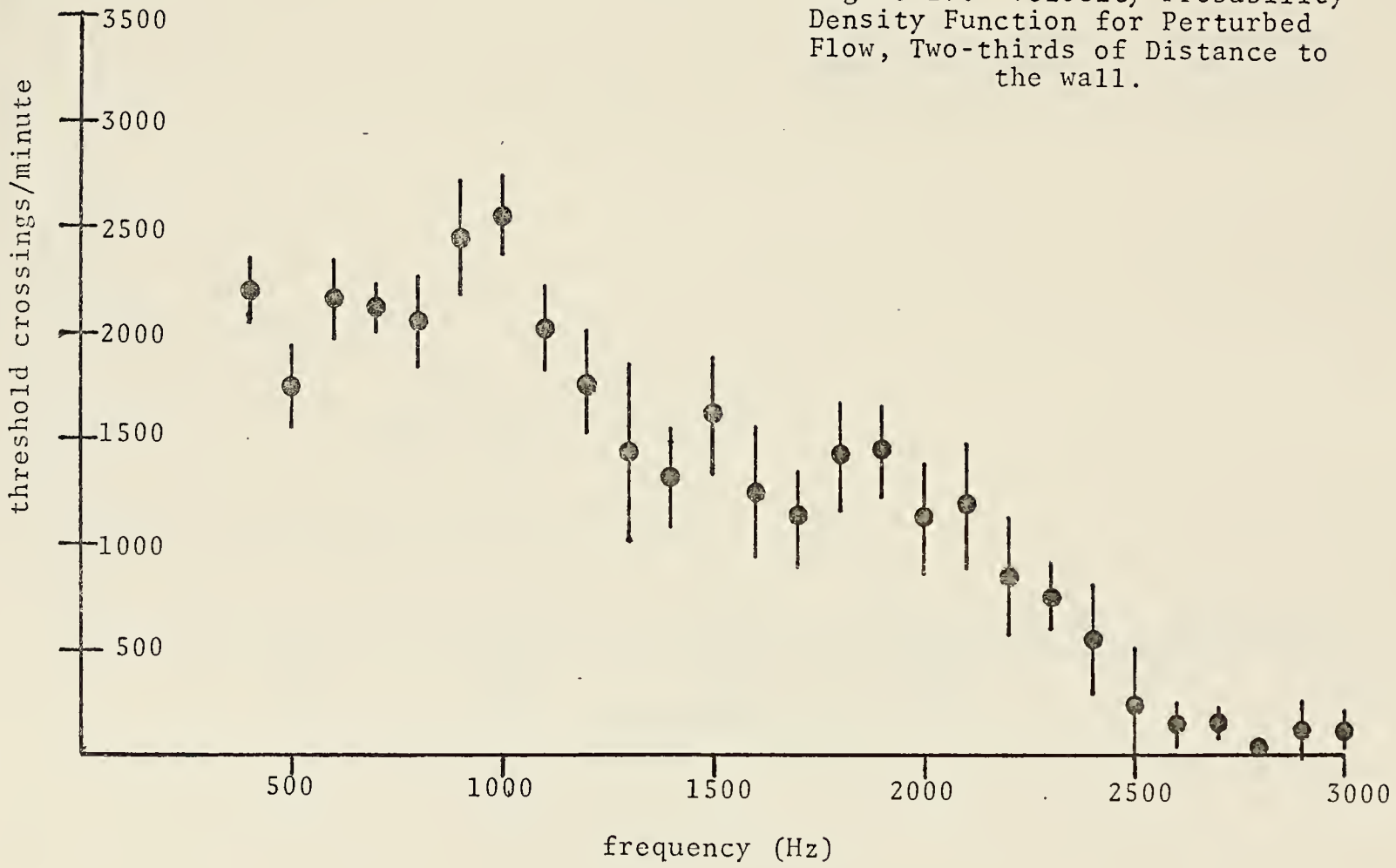

Figure 17. Velocity Probability Density Function for Perturbed Flow, Two-thirds of Distance to the wall.

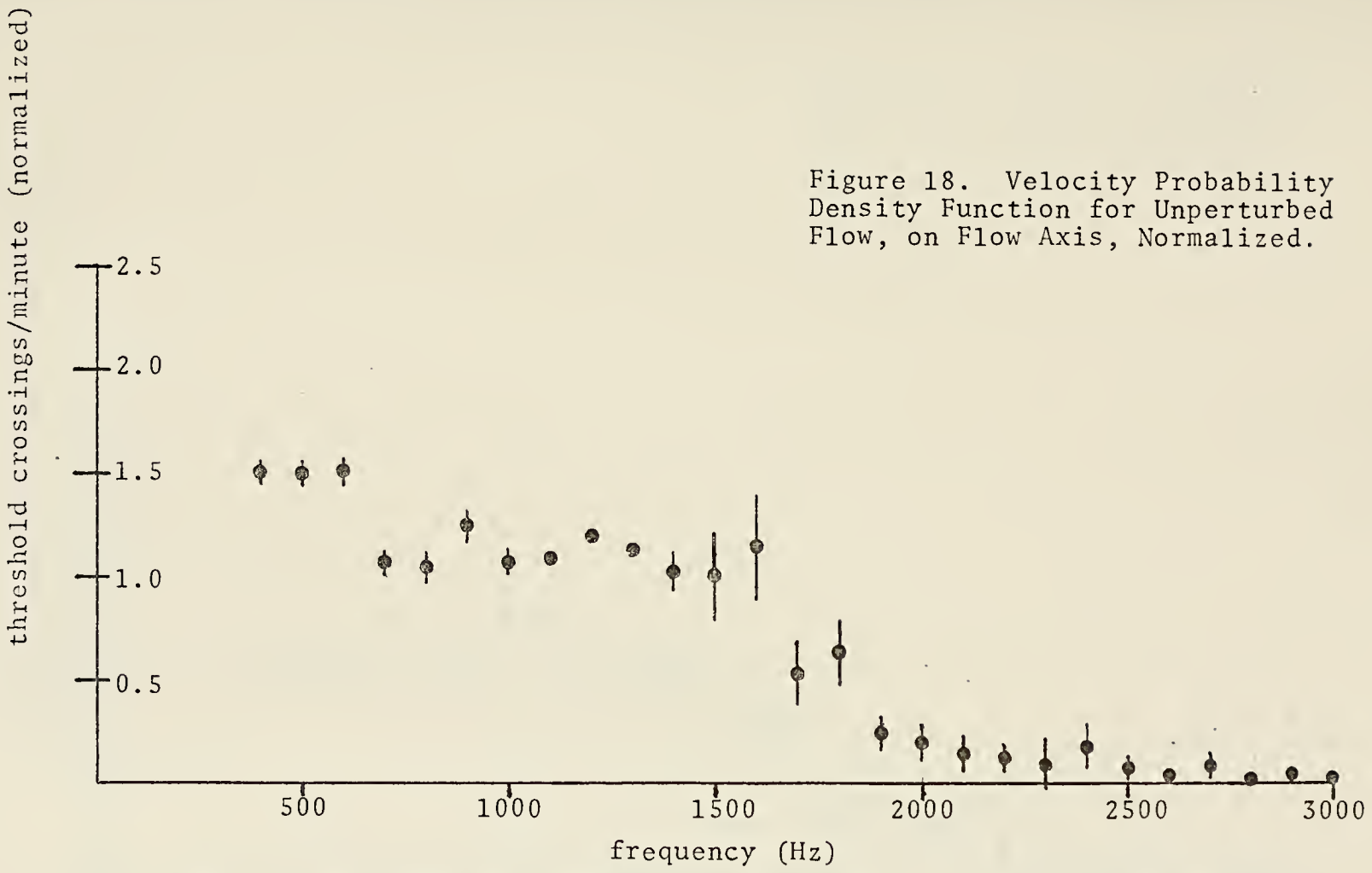

Figure 18. Velocity Probability Density Function for Unperturbed Flow, on Flow Axis, Normalized.

Figure 19. Velocity Probability Density Function for Perturbed Flow, on Flow Axis, Normalized.

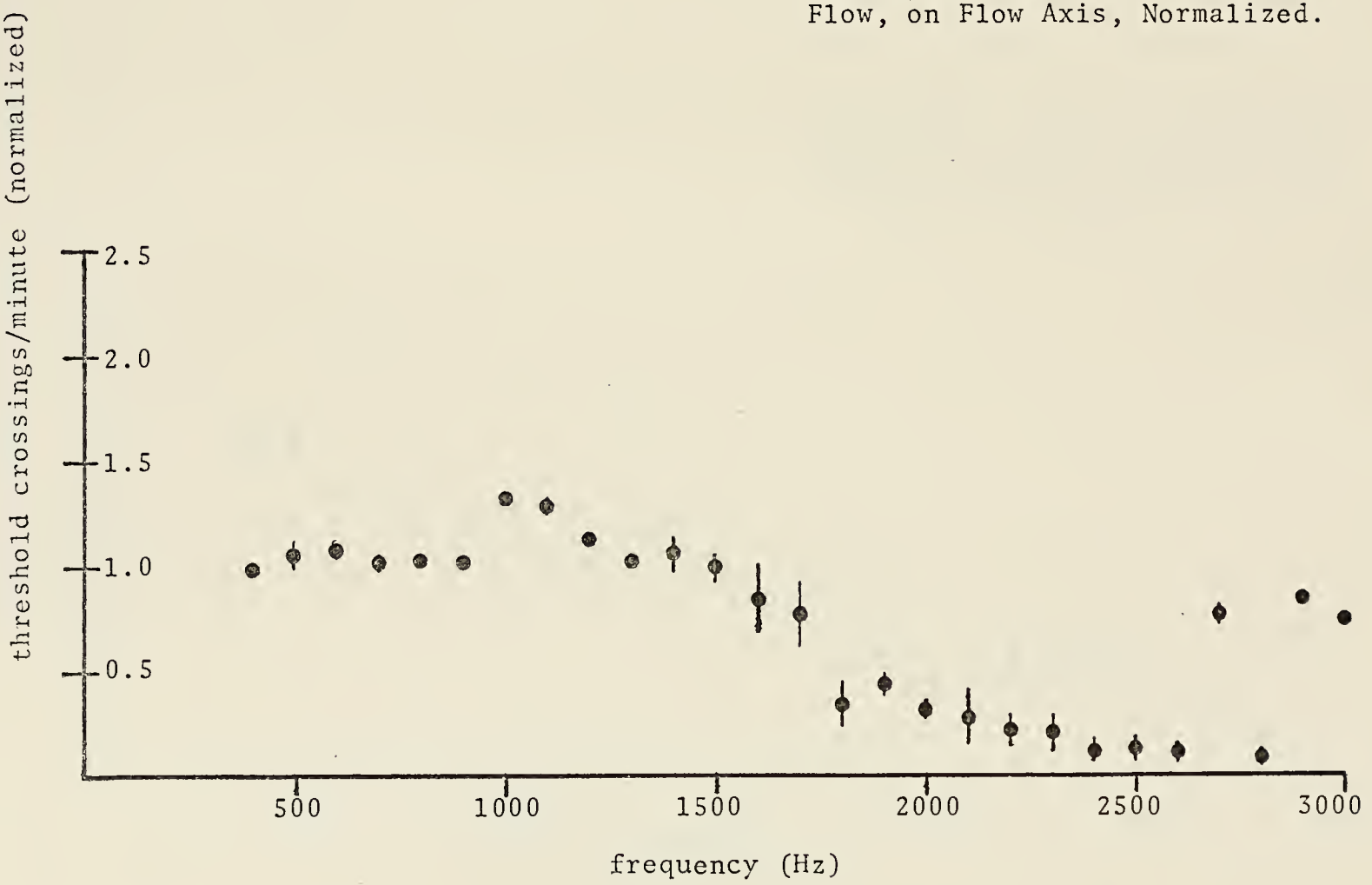

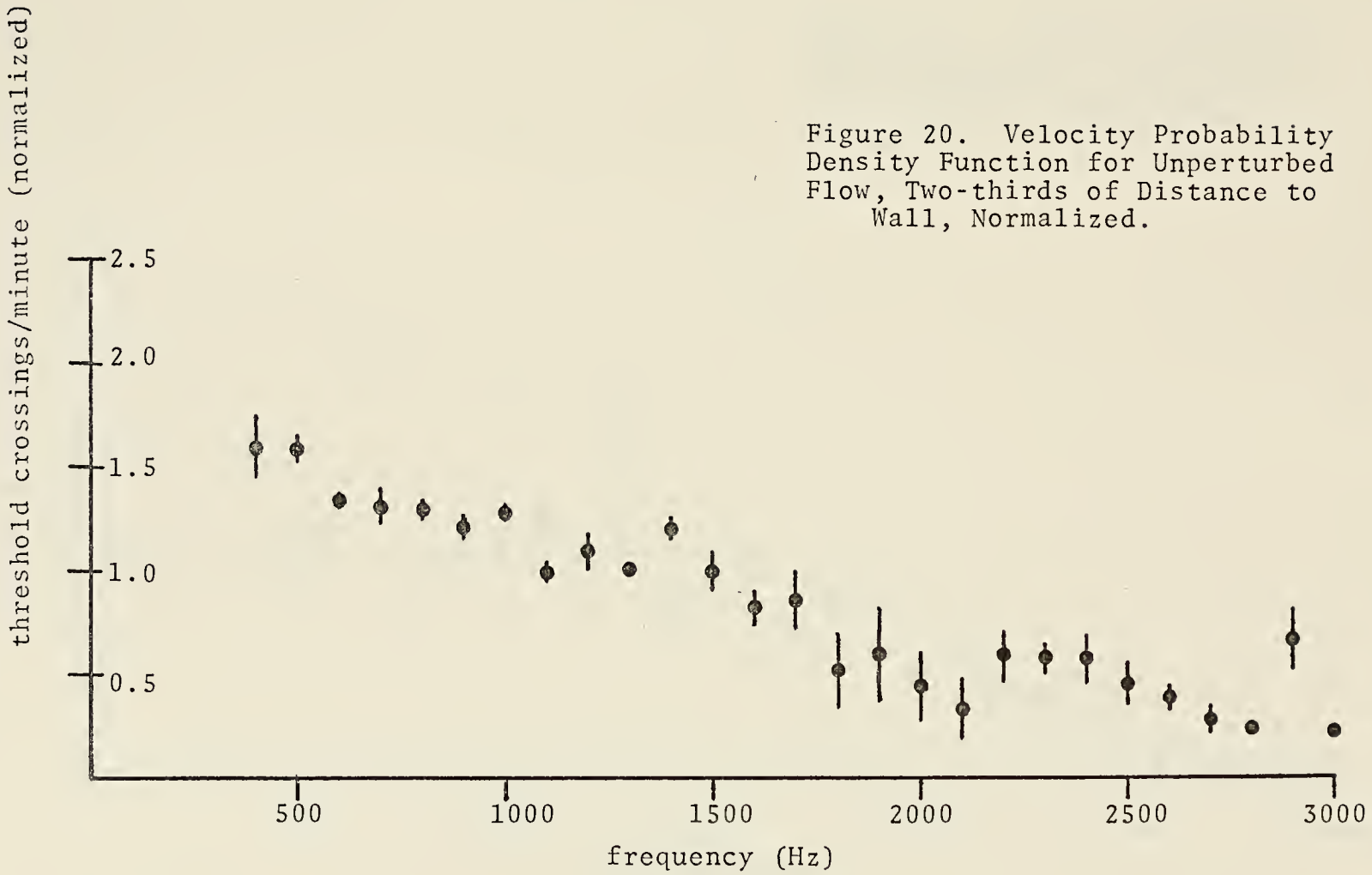

Figure 20. Velocity Probability Density Function for Unperturbed Flow, Two-thirds of Distance to Wall, Normalized.

Figure 21. Velocity Probability Density Function for Perturbed Flow, Two-thirds of Distance to the Wall, Normalized.

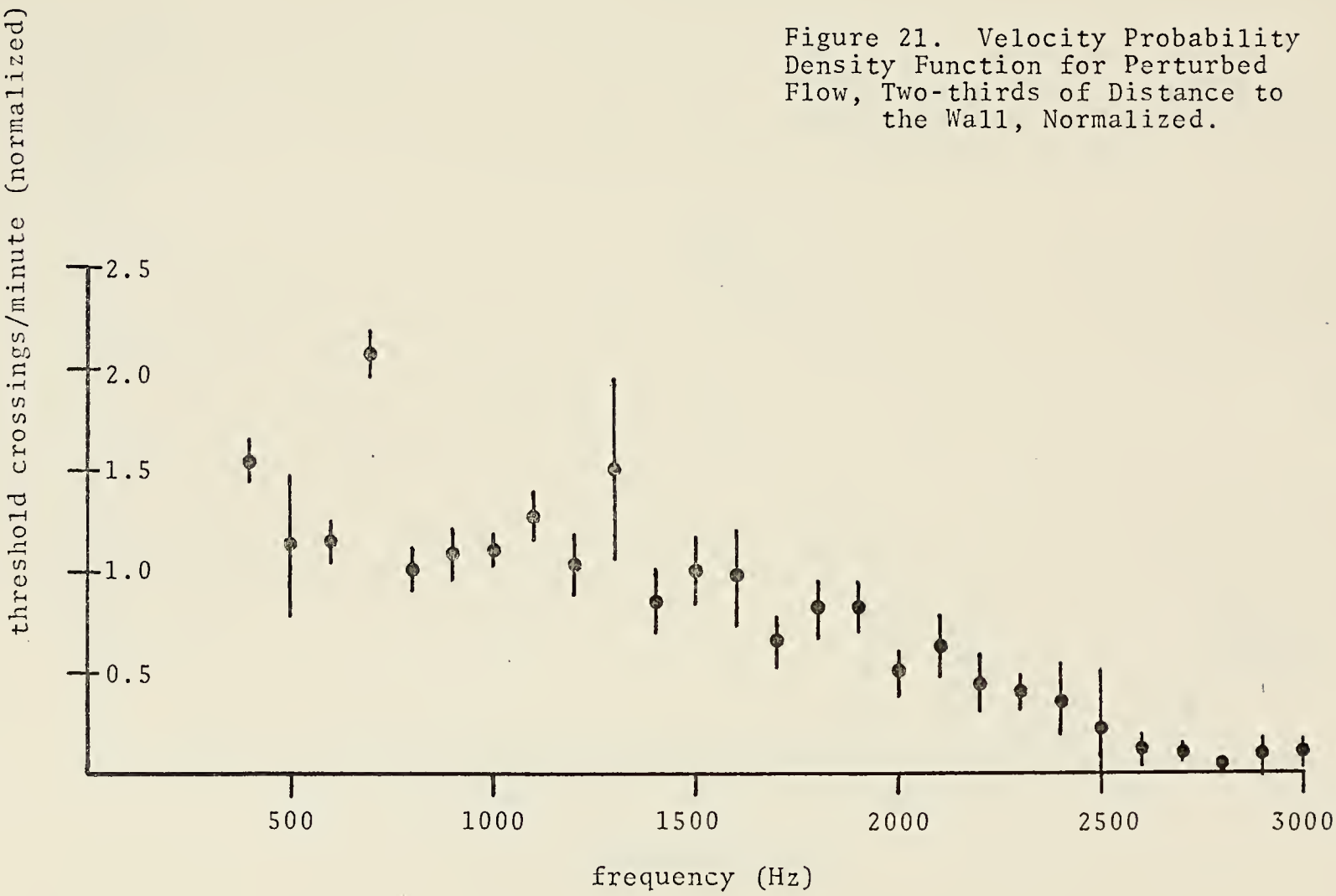

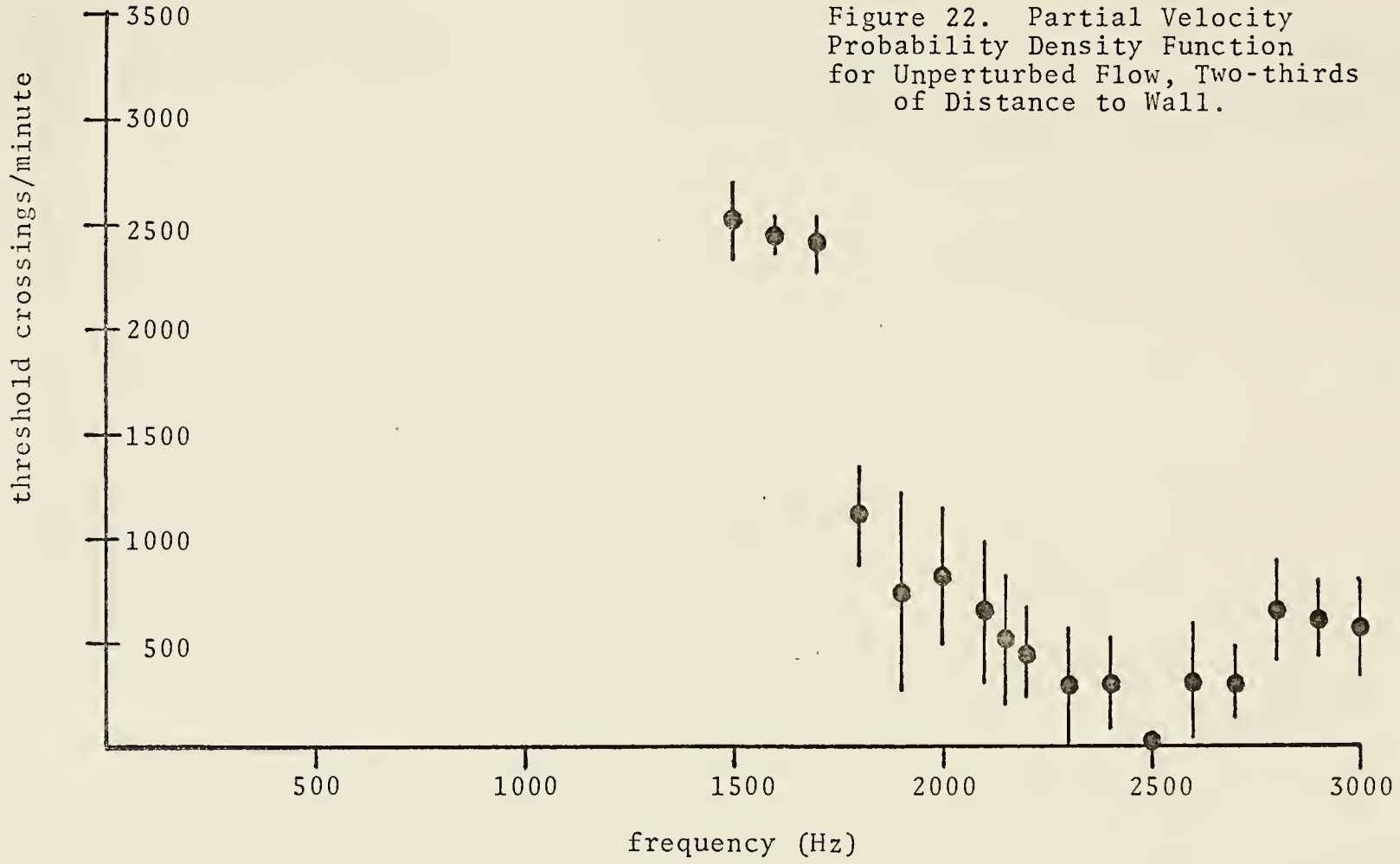

Figure 22. Partial Velocity Probability Density Function for Unperturbed Flow, Two-thirds of Distance to Wall.

Figure 23. Partial Velocity Probability Density Function for Unperturbed Flow, Two-thirds of Distance to the Wall, Normalized.

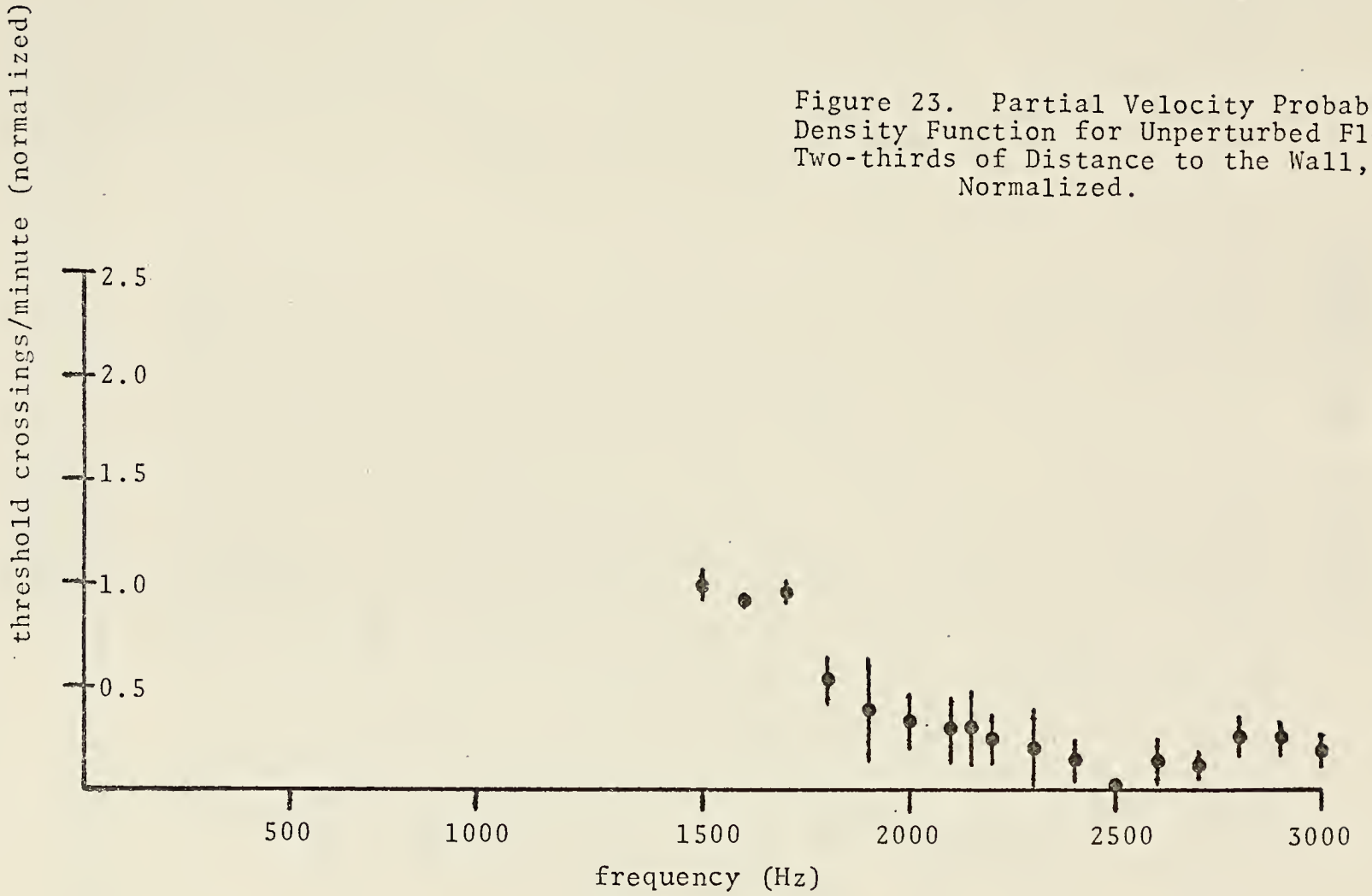

IV. SUMMARY AND CONCLUSIONS

During the course of this experimental study a simple, economical, and functional laser velocimeter system was constructed from readily available components. This system was used in a dual scatter, individual realization mode to measure longitudinal velocities of fluid flowing in a water tunnel. A transparent tunnel of rectangular cross section was designed and constructed which provided a means by which low Reynolds Number fluid flow could be studied with the laser velocimeter. Measurements were made for four different conditions of flow. A method for measuring turbulent velocities was developed and tested whereby the relative occurrence of the frequencies composing the scattered light from the observation region in the fluid was statistically determined.

Special emphasis was placed on developing a simple, but sufficiently sensitive, system which could be refined and modified as necessary for use in future studies. The system described herein could easily be adapted for use in a variety of fluid flow experiments. Detailed information on the design, construction, and operation of the system is provided in the appendices for the benefit of future investigators.

The following is a summary of observations and conclusions based upon the results of this experiment.

1. The construction of a simple, accurate, and reliable laser velocimeter for measuring turbulent fluid flow is feasible. The optics could be made less susceptible to vibrations and misalignments by placing the lenses in shock-resistant mountings.

2. A method for accurately measuring fluid flow characteristics which is independent of the number of light-scattering particles within the observation volume is possible. The procedure employed in this experiment, wherein the relative occurrence of the frequency components of the scattered light signal was measured, gives a meaningful velocity distribution. It could be improved by simultaneously recording the strength of the scattered light signal at the frequency under observation and the strength of the signal at a preselected standard frequency in order to account for changes in particle density in the observation region.

3. The velocity resolution of the profiles obtained by this method is highly dependent upon the geometry of the velocimeter optical arrangement. In particular the width of the beam crossing region should be minimized in order to reduce the spread in the number of fringe crossings per realization, and in order to improve spatial resolution so that more detailed measurements could be made. The size of particles within the flow should be smaller than the fringe spacing of the beam crossing intensity pattern in order that low frequency components of the photomultiplier signal

which are not truly representative of the flow velocities may be eliminated.

4. Studies of low velocity flow are inherently difficult because of the proximity of the low frequency spectral components of the scattered light associated with the size and crossing angle of the laser beams. At low velocities these low frequency components interfere with the components of the signal related to flow velocity. Thus filtering is more difficult. A water tunnel which features laminar flow at higher velocity is desirable for future studies. Modification of the present tunnel by placing flow straighteners at the entrance to make the flow laminar, and by shaping and enlarging the outlet to avoid backup disturbance would perhaps be sufficient.

5. The array of signal processing equipment used, while adequate for this study, nevertheless did require an excessive amount of time for data collection. This time could be reduced significantly by use of a multi-channel analyzer with automatic signal recording.

6. The laser velocimeter offers a potentially superior method of making flow measurements due to its obvious advantage that the flow need not be disturbed by the measuring probe. Care must be taken, however, to ensure that the effects of factors not related to the flow are identified and quantified.

APPENDIX A

THE FLOW SYSTEM

The complete flow system used in this experiment is shown in Figure 24. A 48 in. x 6 in. x 6 in. (inner dimensions) water tunnel, Figure 25, was constructed of 1/2 in. transparent Lucite sheeting bonded with trichloroethylene. The tunnel was securely attached to the inlet piping by means of a 1/2 in. thick Lucite flange which was bolted to an aluminum collar at the end of the inlet pipe. An O-ring inserted in the flange prevented leakage. Two access ports from which different test shapes could be suspended were provided in the top surface of the tunnel. The ports, also made of Lucite, were machined to fit flush with the inner surface of the tunnel, thus preventing unwanted flow distortion. O-rings were used to prevent leakage. The outlet of the tunnel was fitted with a one in. diameter pipe (fitted with a 3/4 in. globe valve) to which the drain hose was attached.

It is important to note here that while the inlet of the tunnel was tapered, the outlet was not. While turbulence generated at the outlet by the sharp reduction in flow cross sectional area did not appear to extend back to the middle of the tunnel where measurements were made, future consideration should nevertheless be given to tapering the outlet end of the tunnel as well. Consideration should also be

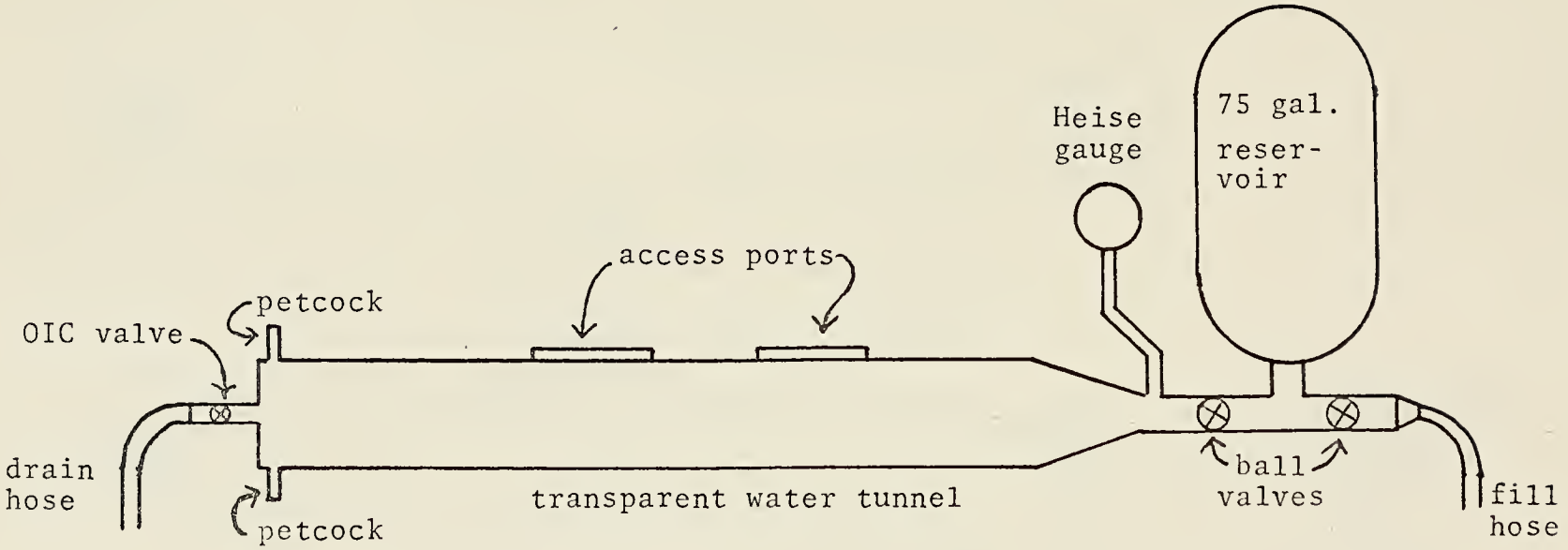

Figure 24. Complete Flow System

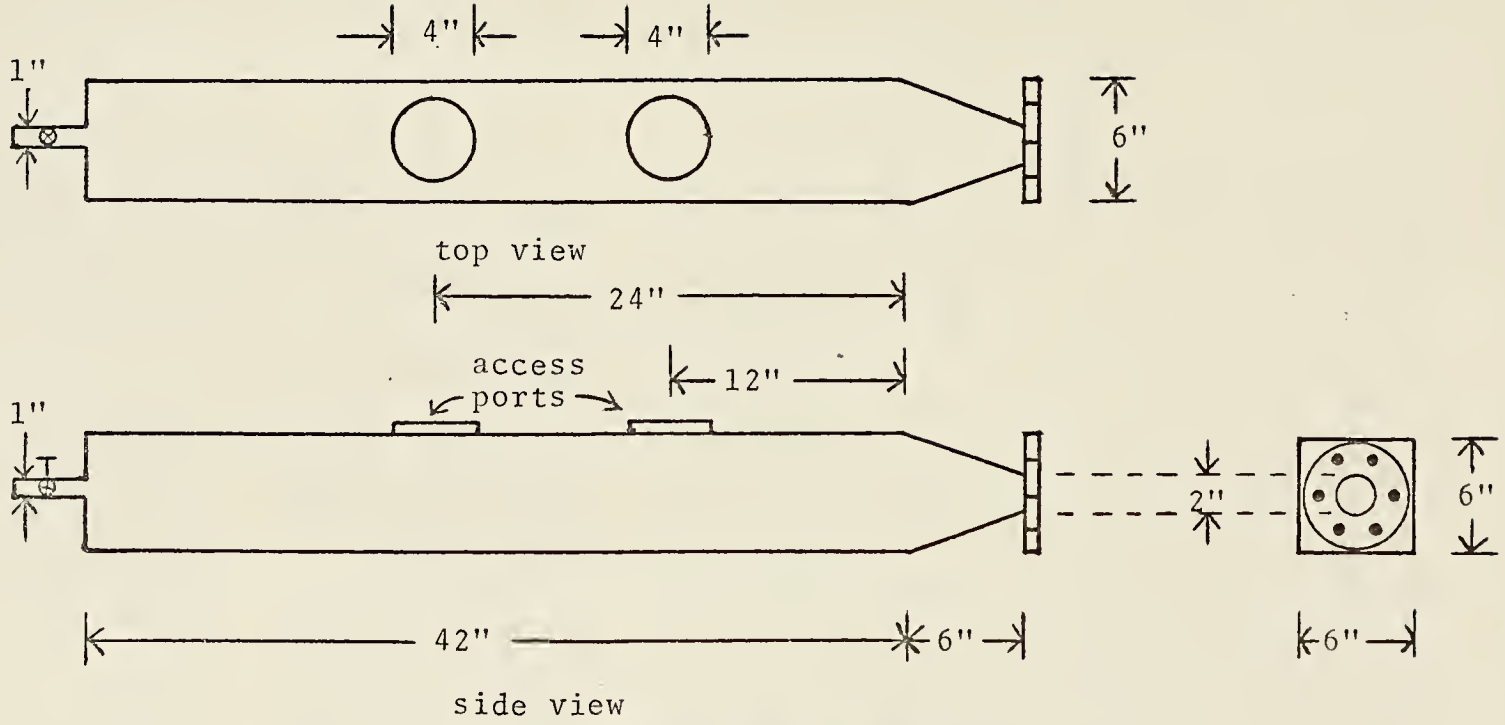

Figure 25. Water Tunnel Dimensions.

given to enlarging the outlet pipe to equal the size of the inlet (two in. ID) in order to increase the mean flow velocity.

As constructed, the inlet region of the tunnel proved to be a significant source of unwanted turbulence because of the sudden transition of the flow from a circular pipe to a square tunnel. Due to machining limitations, a smooth transition of cross sectional area from circular to square could only be approximated. After construction was completed, caulking compound was used to fill in the corners of the inlet region of the tunnel in order to give the region a more rounded shape, but this reduced the turbulence only marginally. In future experiments, consideration should be given to placing flow straighteners, such as straws, at the inlet end of the tunnel to make the flow more nearly laminar.

The flow medium used was ordinary tap water fed to the tunnel through a reservoir system used in a previous experiment. No attempt was made to seed the water since preliminary experiments had demonstrated that enough particulate matter was always present to ensure a good signal. Conversely, no attempt was made to filter the water.

A seventy-five gallon stainless steel tank was used only as a reservoir to hold excess water during periods of data collection. In future experiments, however, the tank could be used to hold a mixture of drag-reducing agent and water in a closed-cycle recirculation system.

A two in. (ID) pipe equipped with two two-in. ball valves transferred the fluid from the fill hose to the inlet of the water tunnel. The flow rate in the tunnel could be controlled by the inlet and outlet valves; however, in this experiment, all observations were made at essentially the maximum flow rate with both valves open. A Heise bourdon-tube pressure gauge (Model CMM) was attached to the two in. pipe to monitor the pressure at the entrance of the tunnel.

APPENDIX B

THE LASER VELOCIMETER OPTICAL SYSTEM

A schematic diagram of the laser velocimeter optical system is shown in Figure 26. The optics of the system were mounted on a one meter optical bench placed beneath and perpendicular to the water tunnel. The optical axis had to be perpendicular to the tunnel axis so that the longitudinal component of fluid velocity would be measured. A 1.8 milliwatt C. W. Radiation Helium-Neon laser was used as the light beam source. The beam from the laser was projected onto the apex of a biprism mounted at the 0-cm. mark of the bench. The biprism split the laser beam into two diverging beams of equal intensity. These beams were made parallel by a 52 cm focal length converging lens (L1) placed on the optical axis 30 cm forward of the biprism. A ten cm focal length converging lens (L2) in front of the water tunnel was used to focus the two beams so they crossed at the desired observation point within the flow. After passing through the tunnel, the two beams were blocked by a mask with a 0.4 cm hole in its center so that only the light scattered forward from the probe volume was focused onto the head of a Dumont (Model 6291) photomultiplier tube by a two cm focal length converging lens (L3). The photomultiplier was biased by an NJE D.C. Power Supply (Model S-325).

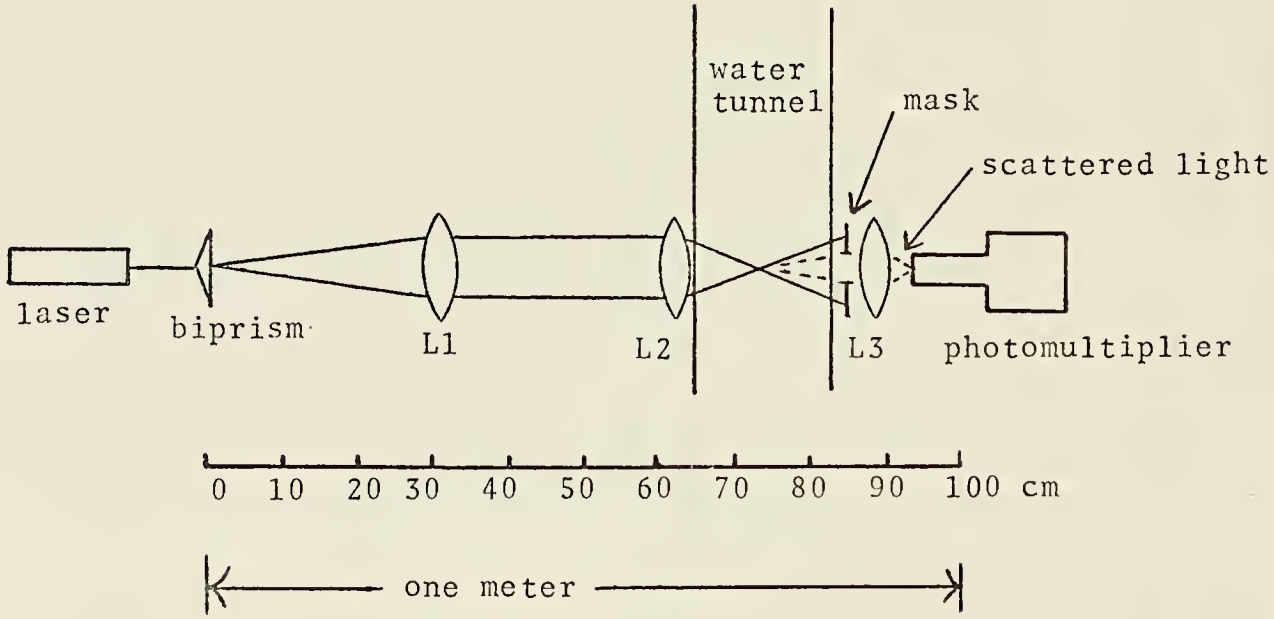

Figure 26. Detailed Arrangement of Laser Velocimeter Optical System (Top View)

The point in the flow at which the two beams crossed was determined by the position of lens L2. Since it operated on beams that were parallel, lens L2 could be moved along the optical axis to position the crossing point anywhere across the flow without changing the geometry of the system. The mask was affixed to the front of lens L3, and lenses L2 and L3 were moved in tandem so that the system was always properly aligned.

Because of the refraction of light when passing from the air through the tunnel wall into the water, the movement of the crossing point did not correspond to the movement of lens pair L2 and L3. However, as shown by Blake [Ref. 13], the motion of the intersection point within a fluid of refractive index n is related to the motion of lens L2 by a factor $\sqrt{\{(1-\sin^2\theta/2)/(n^2-\sin^2\theta/2)\}}$ and is independent of the thickness and refractive index of the wall. Therefore, the position of the crossing point within the fluid can be accurately determined once a reference point has been established. A reference scale was determined by noting the positions of the lens L2 when the beams were crossed exactly at the inner wall of each side of the tunnel and then calibrating the distance between these two positions to agree with the actual wall-to-wall distance of the tunnel (six in.).

APPENDIX C

EXPERIMENTAL PROCEDURES

First the tunnel was completely filled with water. Air bubbles were eliminated by tilting the outlet end of the tunnel slightly above the horizontal plane as it was being filled so that air would be allowed to escape through a petcock located on the top surface of the tunnel at the outlet end. The outlet valve was then opened fully and the inlet ball valve was opened so that the tunnel would be completely full at all times. The mean flow rate was measured at the beginning of each run to ensure that the mean flow velocity was the same for all runs. During each run, the inlet pressure was monitored and the ball valve at the inlet adjusted if necessary to keep the flow constant. Excess water was allowed to accumulate in the reservoir. The system was allowed to run for at least fifteen minutes before measurements were taken in order to eliminate any large particulate residue (rust, caulk flakes, etc.) from the flow.

The laser velocimeter optics were then checked to see that the beams were of equal intensity and that they actually crossed at the desired observation point in the flow. The position of the photomultiplier tube was adjusted to provide a maximum signal-to-noise ratio as indicated by the Hewlett-Packard oscilloscope.

The wave analyzer was set for a maximum input voltage of 0.3 volts, a range of three millivolts, and the NORMAL mode with AFC was used. The output amplitude was set at maximum.

After amplification, the restored frequency output of the wave analyzer for all frequencies to be observed was found to vary between zero and approximately four volts (peak). The trigger level of the Tektronix oscilloscope was therefore set to a median level of two volts (peak). For every excursion of the wave analyzer output above two volts (peak), the oscilloscope would trigger an eight volt pulse of the shape shown in Figure 27. This pulse in turn was sent to the counter which was set to count all positive voltage excursions above five volts. The counter therefore counted every pulse from the oscilloscope.

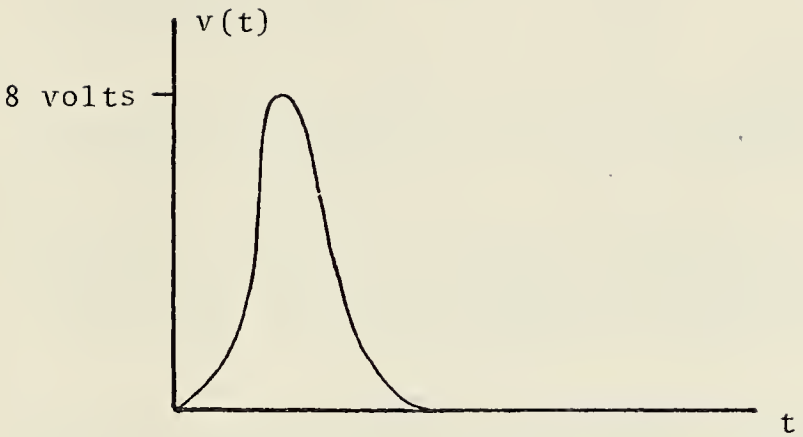

Figure 27. Trigger Pulse to Counter.

LIST OF REFERENCES

1. Rudd, M. J., "The Laser Anemometer--A Review," Optics and Laser Technology, p. 200-207, November 1971.

2. Yeh, H., and Cummins, H. Z., "Localized Fluid Flow Measurements with the He-Ne Laser Spectrometer," Applied Physics Letters, v. 4, p. 176, 1964.

3. Foreman, J. W., Jr., George, E. W., Felton, J. L., Lewis, R. D., Thornton, J. R., and Watson, H. J., "Fluid Flow Measurement with a Laser Doppler Velocimeter," IEEE Journal of Quantum Electronics, QE-2, p. 260-266, 1966.

4. Rudd, M. J., "A Self-Aligning Laser Doppler Velocimeter," Optical Instruments and Techniques, Oriel Press, p. 158-166, 1969.

5. Greated, C., "Measurement of Turbulence Statistics with a Laser Velocimeter," Journal of Physics, E: Scientific Instruments, v. 3, p. 158-160, 1970.

6. Edwards, R. V., Angus, J. C., French, M. J., and Dunning, J. W., Jr., "Spectral Analysis of the Signal from the Laser Doppler Flowmeter: Time Independent Systems," Journal of Applied Physics, v. 42, no. 2, p. 837-850, 1971.

7. Wang, C. P., "Instantaneous Turbulence Velocity Measurements by Laser Doppler Velocimeter," Applied Physics Letters, v. 20, no. 9, p. 339-341, 1 May 1972.

8. Oklahoma State University, School of Mechanical and Aerospace Engineering Report ER 72-F-11, Turbulence Measurements with a Laser Anemometer Measuring Indivual Realizations, by G. L. Donohue, D. K. McLaughlin, and W. G. Tiederman, November 1971.

9. Schlichting, H., Boundary Layer Theory, p. 591-604, McGraw-Hill, 1960.

10. Daily, J. W., and Harleman, D. R. F., Fluid Dynamics, p. 386, Addison-Wesley, 1966.

11. Goldstein, R. J., and Kreid, D. K., "Measurement of Laminar Flow Developed in a Square Duct Using a Laser Doppler Flowmeter," Journal of Applied Mechanics, v. 34, p. 813-818, 1967.

12. Hill, C. C., III, An Investigation of the Parameters Necessary to Measure Fluid Flow with a Laser Velocimeter, M.S. Thesis, U. S. Naval Postgraduate School, Monterey, 1974.

13. Blake, K. A., Development of the NEL Laser Velocimeter, paper presented at International Conference on Modern Developments in Flow Measurement, Harwell, 21-23 September 1971.

INITIAL DISTRIBUTION LIST

		No. Copies
1.	Library, Code 0212 Naval Postgraduate School Monterey, California 93940	2
2.	Department Chairman, Code 61 Department of Physics and Chemistry Naval Postgraduate School Monterey, California 93940	2
3.	Professor K. E. Woehler, Code 61 Wh Department of Physics and Chemistry Naval Postgraduate School Monterey, California 93940	4
4.	Assoc. Professor J. V. Sanders, Code 61 Sd Department of Physics and Chemistry Naval Postgraduate School Monterey, California 93940	1
5.	LCDR Robert Blakeley Yule, USN 41 Warren Street Somerset, Massachusetts 02726	1